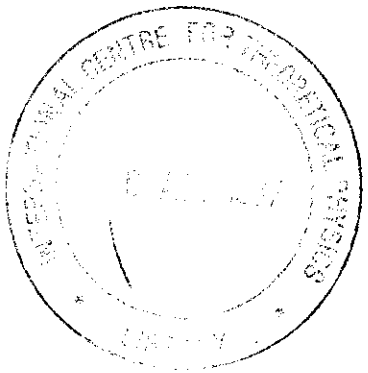

INTERNATIONAL ATOMIC ENERGY AGENCY
UNITED NATIONS EDUCATIONAL, SCIENTIFIC AND CULTURAL ORGANIZATION

INTERNATIONAL CENTRE FOR THEORETICAL PHYSICS
34100 TRIESTE (ITALY) - P.O.B. 586 - MIRAMARE - STRADA COSTIERA 11 - TELEPHONE: 2240-1
CABLE: CENTRATOM - TELEX 460392 - 1

H4.SMR/204 - 27

WINTER COLLEGE ON

ATOMIC AND MOLECULAR PHYSICS

(9 March - 3 April 1987)

COMBUSTION DIAGNOSTICS

M. Alden

Lund Institute of Technology
S-221 00 Lund
Sweden

V. COMBUSTION STUDIES USING LASER TECHNIQUES

Ten years elapsed after the invention of the laser in 1960 before it was used in combustion probing. The Raman technique was first used in this context, since it did not require any tunable laser. Much of the early work on laser applications in combustion diagnostics was presented in a conference proceedings in 1974 [82]. As the tunability of the laser became larger, and doubling and mixing processes allowed further wavelength extensions, the laser-induced fluorescence (LIF) and Coherent anti-Stokes Raman Scattering (CARS) techniques became important in combustion diagnostics. The numbers of combustion meetings presenting papers on laser techniques were rapidly growing in the second half of the seventies, see e.g. [83-86]. A comprehensive review of the applications of laser diagnostic techniques was written in 1979 by Eckbreth et al. [87], and recently the field was reviewed by Bechtel and Chraplyvy [88]. In this chapter most attention is paid to laser-induced fluorescence, Raman spectroscopy and CARS, since these techniques have proved to be very important tools in combustion diagnostics. Other laser techniques, both spectroscopic, such as absorption and optogalvanic, and non-spectroscopic, such as laser Doppler anemometry and elastic scattering (Mie and Rayleigh scattering), are also valuable and will be briefly reviewed in a final section.

V.1 Laser-Induced Fluorescence (LIF)

Laser-induced fluorescence (LIF) is based on laser excitation of atoms or molecules from the ground state to an excited state. After a short time the atom/molecule reemits radiation. This radiation can be analyzed and information on both temperatures and concentrations can be deduced. Since the ground state, responsible for the excitation, is definite and the fluorescence from the corresponding upper state also occurs from definite vibrational and rotational levels, the selectivity using LIF is considerable. This selectivity combined with high sensitivity makes LIF a very powerful diagnostic tool.

Until recently, the LIF technique was limited to atoms and molecules with absorption bands accessible to lasers, but using the two-photon absorption technique even species with absorption bands in the VUV can now be detected, as will be discussed more later. During the last few years several review articles describing the LIF techniques applied to combustion diagnostics have appeared, e.g. Refs. [89-91].

A typical experimental set-up for a LIF experiment is shown in Fig. V.1. The dye laser beam is focused in the flame and the

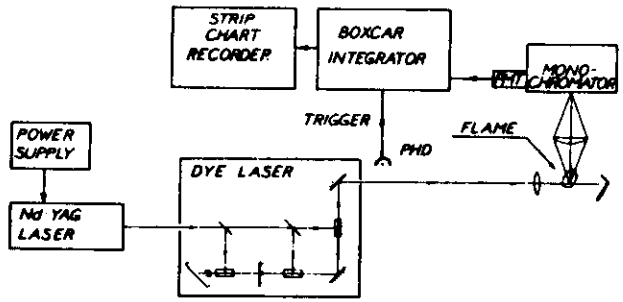

Figure V.1 . Experimental set-up for a laser-induced fluorescence experiment.[c]

fluorescence light is collected at right angles. There are essentially two methods of acquisition of the fluorescence spectrum, which are described in Fig. V.2. The approach shown in Fig. V.2a, where the laser frequency is scanned through the absorption region of the molecule, is called excitation spectroscopy. Here the fluorescence is detected using a broadband filter. An excitation spectrum is similar to an absorption spectrum, with the advantage of detecting the fluorescence light against a null background. Exampels of excitation spectra are given in Figs.

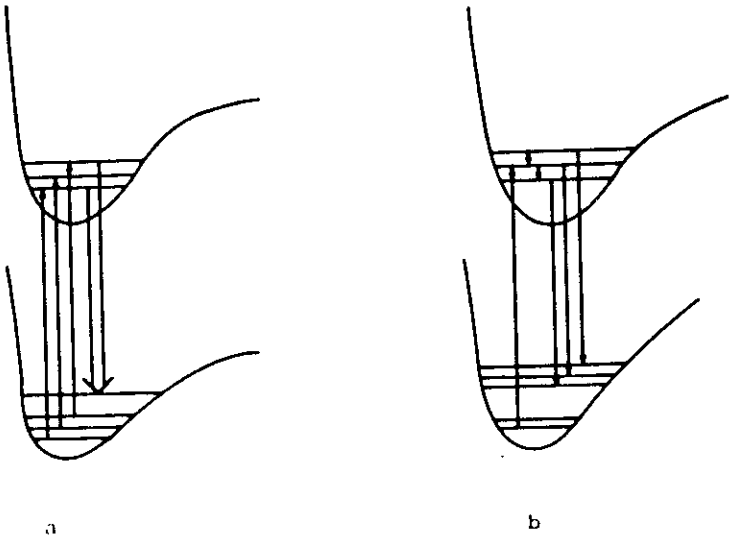

Figure V.2 . a) The principle of excitation spectroscopy, b) The principle of fluorescence spectroscopy.

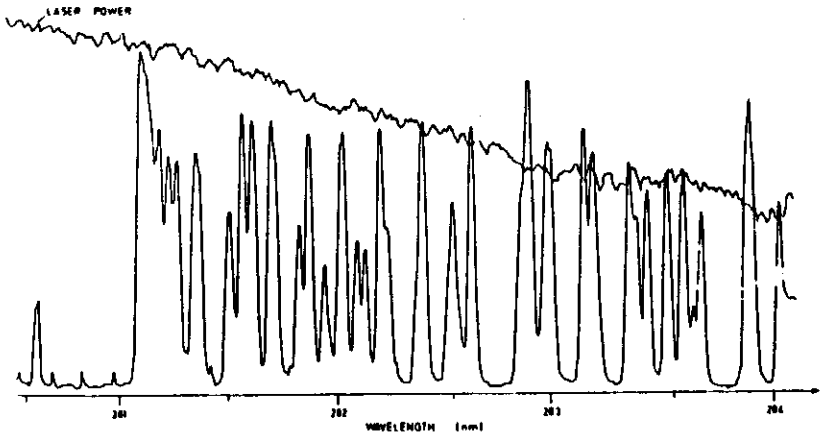

Figure V.3 . Excitation spectrum of the OH radicals in a propane/air flame.[c]

V.3 and 4. Fig. V.3 shows an OH spectrum, which was realized using the tracking device described in Chapter IV. In Fig.V.4 an other example of an excitation spectrum is shown, now for C_2 radicals. The other type of fluorescence

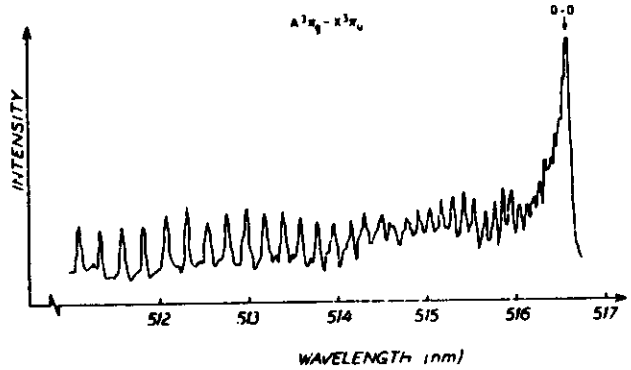

Figure V.4 . Excitation spectrum from C_2 radicals in a propane/air flame. [c]

spectrum, illustrated in Fig. V.2b) is obtained when using a fixed laser wavelength to excite a specific level of the molecule. Then the resulting fluorescence spectrum is recorded through scanning a monochromator. A fluorescence spectrum of CN is shown in Fig. V.5. Here a specific wavelength is pumped and through collisional energy transfer other levels are also populated and emit radiation.

The resolution of an excitation spectrum is given by the laser source, whereas for a fluorescence spectrum the resolution is set by the monochromator used. Several molecules of interest in combustion chemistry have been detected using one-photon LIF. In Table V.1 these molecules,mainly intermediate radicals, are listed. In addition to the species listed in Table V.1 Muller et al. have investigated the chemistry of sulfur in rich $H_2/O_2/N_2$ flames and have thus shown LIF from S_2, SH, SO and SO_2 [125].

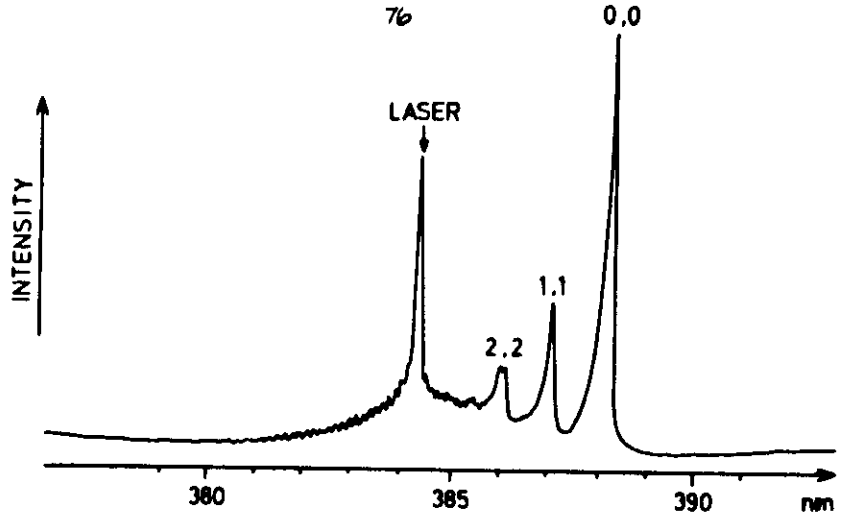

Figure V.5 . Laser-induced fluorescence spectrum from CN radicals in a acetylene/nitrous oxide flame [92].

Table V.1 . Molecules of interest in combustion chemistry, and the corresponding absorption wavelengths together with references.

Molecule	Abs. wavelength (nm)	Ref.
OH	~306	22,93-94
C_2	~516	101,102,105-111
CH	~431	101,102,108,112-115
CN	~388	101,102,113,115
NH	~336	22,101,103,116
NO	~226	101,115-117
NCO	~399, ~466	118,119
NO_2	450-470	120
C_3	405	121
CH_2O	320-345	122
C_2O	657-677	123
NH_2	430-900	124

V.1.1 Concentration Measurements

The application of LIF for concentration measurements is very wide and as already has been pointed out, the sensitivity is high. E.g, Na atoms at concentrations down to 10^4 atoms/cm^3 have been measured for atmospheric-pressure flames [126].

The fluorescence power S_F from an upper level with the population N_2 is given by

$$S_F = \frac{hc}{\lambda_F} \frac{A_{21}}{4\pi} \Omega V N_2 \qquad (1)$$

where λ_F is the fluorescence wavelength, A_{21} is the rate for radiative decay, Ω is the light-collection angle and V is the sample volume. In order to relate N_2 to the undisturbed total population N_T, the corresponding rate equations have to be solved. If we for simplicity consider the two-level system shown in Fig. V.6

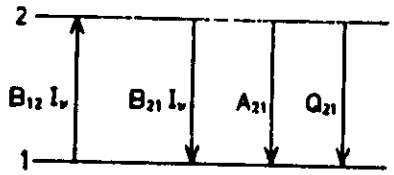

Figure V.6 . A simple model for radiation processes in a two-level system.

the rate equations can be written

$$\frac{dN_1}{dt} = -N_1 B_{12} I_\nu + N_2 (A_{21} + Q_{21} + B_{21} I_\nu) \qquad (2)$$

$$\frac{dN_2}{dt} = N_1 B_{12} I_\nu - N_2 (A_{21} + Q_{21} + B_{21} I_\nu) \qquad (3)$$

where B_{12} and B_{21} are the Einstein coefficients for absorption of radiation and stimulated emission, respectively. I_ν is the laser energy density, and Q_{21} is the non-radiative rate for

eexcitation induced by collisions (quenching). The quenching ignifically reduces the fluorescence signal. Solving (2) and (3) or a steady state condition, i.e $\frac{dN}{dt} = 0$, and noting that $=N_1+N_2$, the result for N_2 is

$$N_2 = \frac{B_{12} I_\nu N_T}{Q_{21}+A_{21}+(B_{12}+B_{21}) I_\nu} \qquad (4)$$

ien (4) is inserted into (1) the resulting fluorescence power

$$S_F = \frac{hc}{\lambda_F} \frac{A_{21}}{4\pi} \Omega V \frac{N_T B_{12} I_\nu}{[Q_{21}+A_{21}+(B_{12}+B_{21}) I_\nu]} \qquad (5)$$

the limit of low laser spectral intensity (5) may be itten

$$S_F = \frac{hc}{\lambda_F} \frac{B_{12}}{4\pi} \Omega V \left(\frac{A_{21}}{Q_{21}+A_{21}}\right) I_\nu N_T \qquad (6)$$

us, the fluorescence intensity is critically dependent on the enching rate Q_{21} through the factor $A_{21}/(Q_{21}+A_{21})$ which is mmonly called the fluorescence yield or Stern-Vollmer factor. r OH $A \sim 1 \times 10^6$ sec^{-1} [127] whereas the quenching rate in pical flame gases at atmospheric pressure exceeds 10^9 sec^{-1} 1], giving a fluorescence yield of only about one part in a ousand. The quenching phenomenon has limited the applicability LIF, but there exist different approaches to avoid this oblem, which are briefly described below.

turation. The saturation technique for avoiding the quenching oblem was first described by Piepmeier [128] and more recently Daily [129]. Following the proposal by Daily, the fluorescence ver at high laser power, i.e. $I_\nu(B_{12}+B_{21}) >> Q_{21}+A_2$ is ven by

$$S_F = \frac{hc}{\lambda_F} \frac{A_{21}}{4\pi} \left(\frac{B_{12}}{B_{12}+B_{21}}\right) \Omega V N_T \qquad (7)$$

ther, since $g_1 B_{12} = g_2 B_{21}$, (g_1 and g_2 are the

degeneracies of level 1 and 2, respectively), the factor $B_{12}/(B_{12}+B_{21})$ can be replaced by $1/(1+g_1/g_2)$.

Early experiments using saturated fluorescence on atoms seeded into a flame were performed by Omenetto et al. [130] and later by Daily et al. [131]. Baronawski et al. [105,107] realized that complete saturation may be difficult to achieve in molecules. Therefore, in their approach S_F in Eq. (5) is Taylor expanded in I_ν^{-1} . The result is

$$S_F \approx \frac{hc}{\lambda_F} \frac{A_{21}}{4\pi} \left(\frac{B_{12}}{B_{12}+B_{21}}\right) \Omega V \left(N_T - \frac{N_T(Q_{21}+A_{21})}{(B_{12}+B_{21})} \cdot \frac{1}{I_\nu}\right) \qquad (8)$$

which is almost identical to the formula given in [107], the only difference is that Baronawski et al. [107] have used $B_{12}/(B_{12}+B_{21}) = 1/2$ in their derivation. If S_F is plotted versus $1/I_\nu$ the intercept leads to N_T, whereas the quenching rate Q_{21} can be determined from the slope. Baronawski et al used this saturation technique for determination of concentrations of C_2 in oxy-acetylene flames. However, the two-level model used by Baronawski et al. is clearly inadequate, since the molecules also possess vibrational as well as rotational structure. In order to interpret data correctly, it is important to account for rotational relaxation during the laser pulse as well as collision-induced rotational and vibrational energy transfer in the upper state. Rotational energy transfer has been examined by many workers, where the OH molecule usually has served as test object [132-134], whereas the vibrational energy transfer has been examined by Lengel et al. [135]. As has been described by Crosley, [136], there are two limiting cases for energy transfer:

a) If the rotational and vibrational transfer rates are much higher than the quenching rate Q, the upper state will thermalize before quenching, resulting in a broad fluorescence spectrum.
b) If the quenching rate Q is much higher than the rotational/vibrational energy transfer rate, only those states coupled by the laser will be populated.

In the case of OH, neither of the two cases applies, and this intermediate situation has been examined by several authors [137-140]. As was pointed out by Verdieck et al. [141] and Berg et al. [138], a very fast rotational redistribution in the lower state means that there are $N_T/2$ molecules in the excited state rather than $N_1^o/2$, which is the case in the absence of any rotational relaxation. (N_1^o is the undisturbed number in state 1 whereas N_T are all molecules.)

Using the saturation techniques, special attention must be paid for avoiding laser-induced chemistry, which was observed by Muller et al. [142] when investigating Na atoms in flames with laser pulses of 2 μs.

Both experimental and theoretical investigations on the influence of the temporal and spatial laser pulse shape on the saturation conditions have been performed [143,144].

Short pulse excitation . This technique for concentration measurement was developed by Stepowski et al. [95,145]. A short laser pulse of duration τ much shorter than the quenching and radiative times is used. It can be shown that the maximum fluorescence power after the laser pulse has terminated is then independent of the quenching rate and rotational relaxation. Due to the restriction on the laser pulse length, this method is only applicable to low pressure flames.

In addition to the two techniques described, another method has been developed by Muller et al. [125], utilizing a calibration procedure. In still another method used by Bechtel et al. [96] the quenching rates are actually calculated, and the number densities from the major collision partners were determined using the Raman technique.

A useful paper has been written by Daily [146], in which uncertainty considerations for LIF such as Rayleigh scattering and trapping effects are discussed.

V.1.2 Temperature Measurements

LIF has also been extensively used for temperature measurements. One technique is to scan the laser frequency across different transitions in e.g. OH followed by a broadband fluorescence detection. This technique for measuring the ground state rotational temperature of OH has been used in e.g. Refs. [147-149]. In another technique, the OH rotational temperature is estimated through excitation of molecules in two different rotational levels in the ground state to the same upper level. By ratioing the fluorescence intensities the temperature can be deduced [150,151]. In yet another technique, the temperature is estimated from the observed rotational [152] and vibrational [153] collisional distributions in the upper electronic state of OH.

So far, only temperature measurements from molecular spectra have been discussed. However, atomic spectra can also be used for the same purpose.
An attractive technique for temperature measurement is to seed a flame with e.g. In, Tl or Ga, and to use the two-line fluorescence technique [156-158]. This technique is further described in Paper 9.

V.1.3 LIF for PAH Measurements

Besides concentration measurements of radicals and temperature measurements, LIF can be used for detection of polyaromatic hydrocarbons (PAH:s) in flames. Since PAH are thought of being important for the soot formation, detection of these species is important. Several groups have used LIF for PAH detection in flames e.g. [159-162].

We have performed a serie of experiments for testing the potential of identification of different PAH:s in flames [163].

)itial experiments were performed using a gas chromatograph (GC))llowed by laser-induced fluorescence detection. Fig. V.7 shows)e resulting chromatogram when feeding the GC with several \H:s, and using a He-Cd laser for excitation. In order

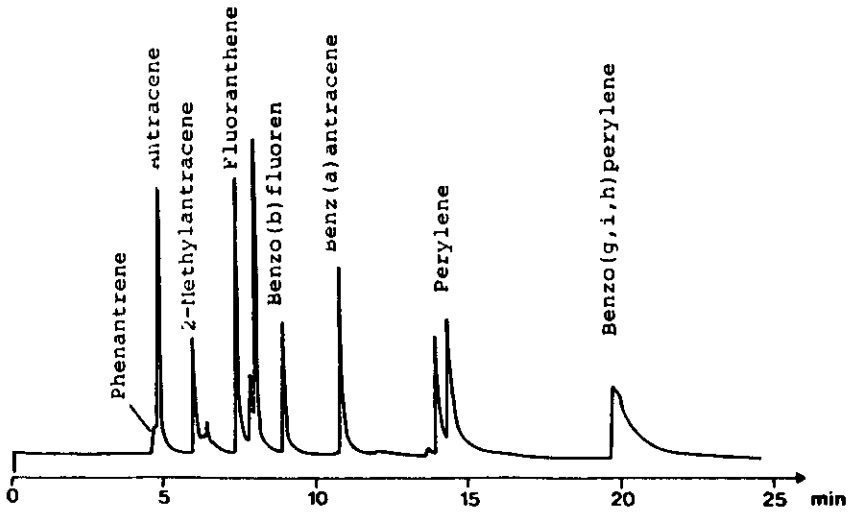

Figure V.7 . Laser-induced fluorescence detection of PAH:s as seperated by a gas chromatograph [163].

) capture the corresponding spectra, a diode array detector was)ed instead of a photomultiplier. For comparing the "cold" PAH)ectra with the flame spectra, certain PAH:s were seeded into a)an flame and the spectra were detected with the diode array)tector. Fig. V.8 shows the fluorescence spectra of different \H:s seeded into the flame, when exciting with a quadrupled YAG)ser beam at 266 nm.

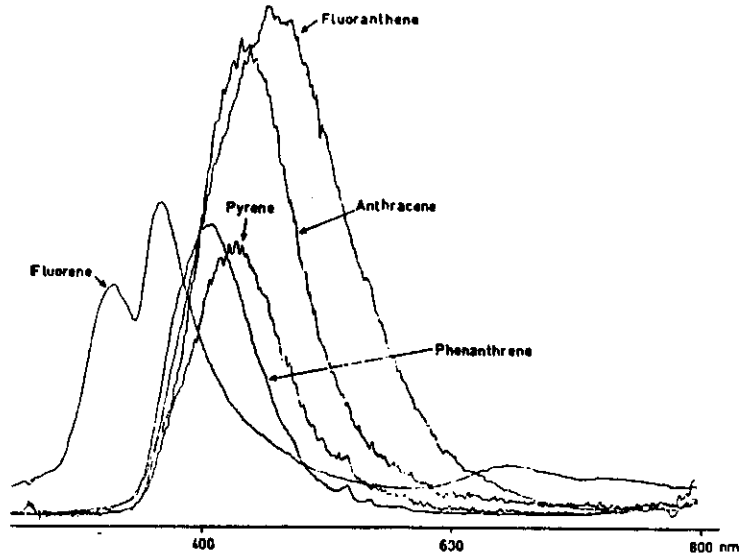

Figure V.8 . Laser-induced fluorescence spectra of different PAH:s seeded into a propane/air flame [163].

V.1.4 Imaging Experiments

All LIF experiments discussed so far have been performed using a photomultiplier tube or a diode array in the dispersive detection mode. However, as was realized in Paper 3, it is possible to use a detector array in an imaging mode, for space-resolved detection of radicals. This Paper describes the space-resolved detection of OH in a methane/air flame. The technique was further developed in Paper 4, where two radicals, C_2 and OH, could be detected simultaneously using two laser systems.

Recently it has been shown by Dr. Crosley's and Dr. Hanson's [164-167] groups at SRI and Stanford University, respectively,

that the technique can be extended to yield information from a plane through the flame.
Fig. V.9 shows the space resolved PAH distribution through a diffusion flame at three different heights above the burner. The fluorescence light was detected through a 10 nm wide interference filter at 405 nm.

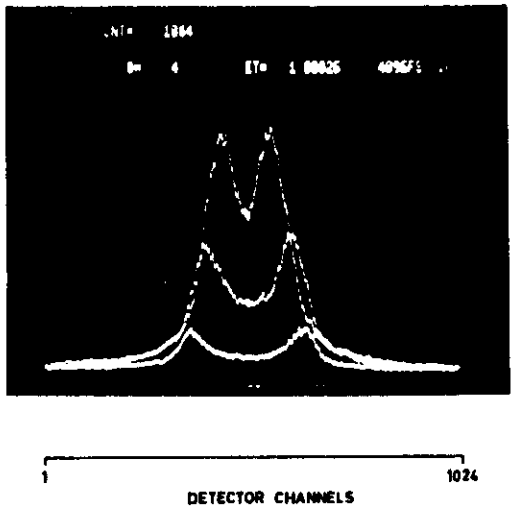

Figure V.8 . Space-resolved PAH distribution at three different heights; 5, 10 and 25 mm above the burner, using a diode array detector.[163]

V.1.5 Two-photon Excitation.

As was indicated in the beginning of this chapter, it has become possible to detect molecules and atoms that normally are undetectable with laser techniques, by using two-photon excitation. Atoms are excited from the ground state to an excited state of the same parity from which fluorescence can be detected in the decay to a lower excited state. In this way it is possible to

detect atoms that absorb in the VUV region. Referring to Chapter III it is appearent that atoms play very important parts in combustion chemistry. The atoms that are most important in this context are shown in Table V.2, where also the excitation

Table.V.2 . Atoms of great importance in combustion chemistry, and their corresponding two-photon wavelengths and detection wavelengths.

Atom	Laser wavelength(nm)	Fluorescence wavelength(nm)
H	206	656
C	280	909
N	211	869
O	226	845
S	308	1046

wavelengths together with the corresponding fluorescence wavelengths are shown. Hydrogen atoms have been detected by two-photon LIF from a DC discharge [168]. Oxygen and nitrogen atoms have been investigated in a similar way by Bischel et al. [169], whereas the first flame detection using two-photon excitation of oxygen is described in Paper 5. Carbon and oxygen atoms have also been detected in a discharge [170].

Molecules have also been detected using two-photon fluorescence. Most experiments have been performed on NO. Although NO may be detected directly, several groups have used two-photon excitation for temperature measurements from the NO spectrum [171,172]. Two-photon excitation of CO has also been reported [173]. An interesting experiment has been performed by Crosley and Smith [174], who detected OH in a flame using two-photon excitation.

.2 Raman Scattering

ıe Raman effect was theoretically predicted in 1923, and first
bserved by C.V. Raman in 1928. With the invention of the laser
ı 1960, the application of Raman scattering became an important
ol for analytical purposes. The big advantages with Raman
cattering are a) quenching does not cause any problem, b)
ıman experiments do not require any tunable laser source, c)
veral species can be measured simultaneously, d) both rota-
onal and vibrational temperature are easily obtained, and e)
oms, radicals as well as molecules that absorb down in the VUV region
measured.
ıfortunately, the Raman effect is very weak, eliminating the
ssibility of measuring small number densities, especially in a
gh-background environment. However, for detection of major
ecies the technique is quite adequate.

veral books describing the Raman effect both theoretically and
perimentally have been published, e.g. [175-180] and its use in
mbustion and flow diagnostics is reviewed in Refs.[181-183].
e theory will here be briefly described followed by sections
scribing temperature and concentration measurements.

2.1 Theory

assically, the Raman effect can be described in terms of the
larizability of a molecule. When a molecule is placed in a
atic electric field, the molecule is distorted . The
sitively charged nuclei and the electrons are attracted towards
e negative and positiv pole of the field, respectively. This
enomenon causes the appearence of an induced electrical dipole
ment, and the molecule is said to be polarized. The induced
ole μ , can be written

$$\mu = \alpha E \qquad (9)$$

ere α is the polarizability of the molecule and E is the

applied field. If E is due to a light wave, e.g a laser pulse, expressed as a travelling wave at frequency ν, amplitude E_o and considering that the molecule undergoes vibrational as well as rotational motions, which change the polarizability periodically, the induced dipole moment for a vibrating molecule can be written

$$\mu = (\alpha_o + \beta \sin 2\pi \nu_R t)\, E_o \sin 2\pi \nu t \qquad (10)$$

where α_o is the polarizability in the equilibrium position, β is the amplitude of the change in the polarizability during the vibration, and ν_R is the vibrational frequency.
Using common trigonometric relations, Eq. (10) can be written

$$\mu = \alpha_o E_o \sin 2\pi \nu t + 1/2\beta E_o \{\cos 2\pi(\nu-\nu_R)t - \cos 2\pi(\nu+\nu_R)\} \qquad (11)$$

Thus, the oscillating dipole has sidebands at frequencies $\nu \pm \nu_R$ in addition to the band at the frequency ν. This classical picture of the Raman effect is qualitatively describing the phenomena, but an examination of a Raman spectrum indicates that for a correct description a quantum mechanical treatment is needed.

Quantum mechanically the incident laser beam of frequency ν consists of photons with the energy $h\nu$, out of which a small part after interactions with the molecules either gain or loose energy, equal to the rotational or vibrational energy-splittings. The elastic scattering is called Rayleigh scattering, whereas the inelastic scattering gives rise to the Raman components. These processes are shown in a schematic energy level diagram in Fig. V.10. The molecules are excited to virtual states, from which they immediately return to a final state emitting photons with an energy equal to the one of the incident photon plus or minus the energy difference between the initial and final state. An examination of the schematic energy level diagram and the corresponding spectrum in Fig. V.10 reveils the structures in a Raman spectrum. The Raman components, where the incident photon has gained or lost energy are called the anti-Stokes and Stokes components, respectively. The selection rules for vibrational

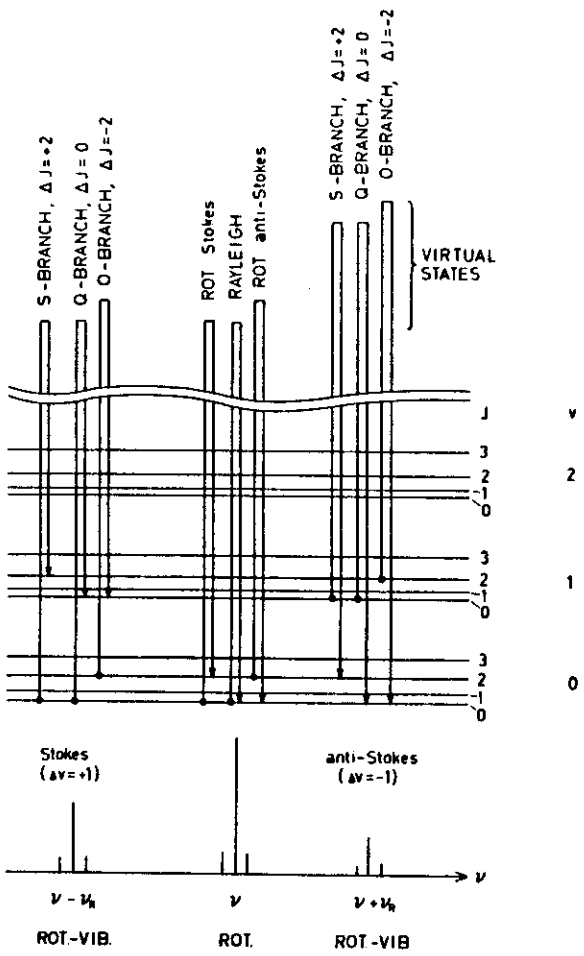

Figure V.10 . Energy level diagram illustrating the Raman effect, where for simplicity only one transition in each branch is shown.

and rotational Raman transitions are $\Delta v = 0, \pm 1$ and $\Delta J = 0, \pm 2$.

Considering the pure rotational Raman spectrum we see that the Rayleigh peak is surrounded by Stokes and anti-Stokes Raman

lines. Recalling from Chapter II, the term value for rotational movement, ignoring the centrifugal distortion, is given by $F(J)=BJ(J+1)$. Considering that the J value can be changed two units, the rotational lines appears at frequencies

$$\nu_{S,AS} = \nu \mp B(4J+6) \qquad (12)$$

Eq. (12) represents a series of equidistant Raman lines, separated by 4B. For a diatomic molecule the number of molecules N_J in the rotational level J of the lowest vibrational state at temperature T is proportional to the Boltzmann factor times the degeneracy

$$N_J \sim (2J+1)\exp[-F(J)hc/kT] = (2J+1)\exp[-BJ(J+1)hc/kT] \qquad (13)$$

The actual number of molecules in a rotational state J is given by

$$N_J = \frac{N}{Q_r}(2J+1)\exp[-BJ(J+1)hc/kT] \qquad (14)$$

where N is the total number of molecules and Q_r is the rotational partition function

$$Q_r = 1+3\exp[-2B\,hc/kT]+5\exp[-6B\,hc/kT]+\ldots$$

Q_r can be replaced by

$$Q_r \approx \int_0^\infty (2J+1)\exp[-hc\,BJ(J+1)/kT]dJ = \frac{kT}{hcB} \qquad (15)$$

In Fig. V.11a N_J is shown as a function of J for different B with fixed T, whereas N_J as a function of J for different T with fixed B is shown in Fig.V.11b. As can be seen the population goes through a maximum for a certain J value, J_{max}, which is given by

$$J_{max} = 0{,}5896\sqrt{\frac{T}{B}} - \frac{1}{2} \qquad (16)$$

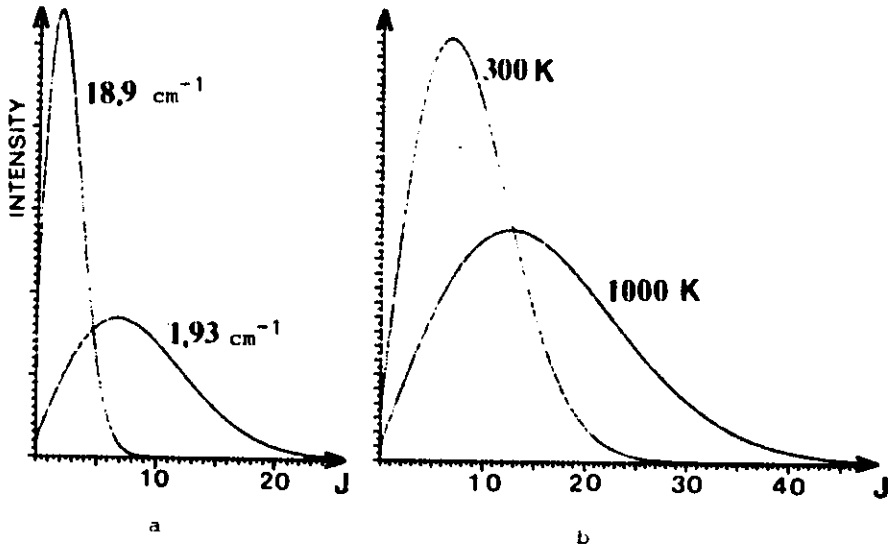

Figure V.11 . a) Plot of N_J for different B values, b) Plot of N_J for different T.

Returning to Fig. V.10, the vibrational transitions occur at $\nu \pm \nu_R$. A vibrational band consists of three branches, the S, Q and O-branch which correspond to $\Delta J = +2, 0$ and -2, respectively. The Raman shifts for the three branches are given by [183]

$$(\nu_R)_S = \Delta\nu_o + 6B_{v'} + (5B_{v'} - B_{v''})\,J + (B_{v'} - B_{v''})\,J^2 \qquad (17)$$

$$(\nu_R)_O = \Delta\nu_o + 2B_{v'} - (3B_{v'} + B_{v''})\,J + (B_{v'} - B_{v''})\,J^2 \qquad (18)$$

$$(\nu_R)_Q = \Delta\nu_o + (B_{v'} - B_{v''})\,J + (B_{v'} - B_{v''})\,J^2 \qquad (19)$$

where $\Delta\nu_o$ is the vibrational frequency shift and $B_{v'}$ and $B_{v''}$ as usual indicate the rotational constant in the upper and lower state, respectively. As is indicated in Fig. V.10, the O-and S-branch are much weaker than the Q-branch, which according to Eq. (19) consists of several very narrow lines since the difference between $B_{v'}$ and $B_{v''}$ is in general very small. As is indicated in the figure, the intensity of the anti-Stokes

lines are, at low temperatures, much weaker than the Stokes ones, since these transitions orginate from excited states. The number of molecules in a vibrational state v is given by

$$N_v = \frac{N}{Q_v} \exp\left[-G_o(v)\, hc/kT\right] \qquad (20)$$

where, as in the rotational case, N is the total number of molecules and Q_v now is the vibrational partition function

$$Q_v = 1 + \exp\left[-G_o(1)\, hc/kT\right] + \exp\left[-G_o(2)\, hc/kT\right] + \ldots \qquad (21)$$

Fig. V.12 a) and b) shows the normalized population density for v=0 and v=1, respectively, for three different molecules, O_2, N_2 and H_2.

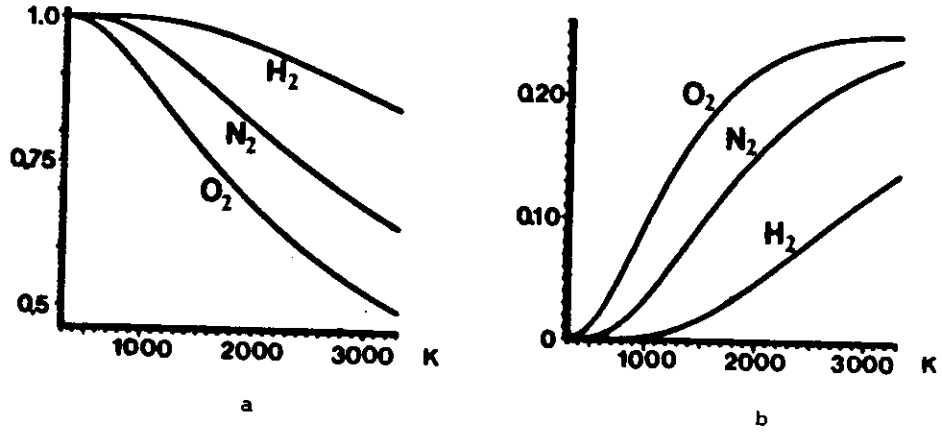

Figure V.12 . a) The normalized population for v=0, b) The normalized population for v=1.

V.2.2 Concentration Measurements

The Raman technique has proved to be a valuable tool for concentration measurements both in exhaust gases and in flames. Rotational Raman scattering is limited for concentration measure-

ments since in a gas mixture, several rotational lines are superimposed. Therefore, this discussion will be limited to vibrational Raman scattering.

The intensity from a vibrational Raman line is given by

$$I = C N I_o \sigma \Omega \ell F(T) \qquad (22)$$

where C is a constant, N the number density, I_o the laser intensity, σ the Raman cross-section, Ω the solid angle, ℓ the length of the observed segment of the laser beam, and F(T) is a temperature dependent factor determined by the spectral width and resolution of the detection system and the investigated molecule. Especially when measuring high-temperature gases, a knowledge of F(T) is a prerequisite for correct concentration measurements. F(T) can be calculated as described by Setchell [184] and Eckbreth [185].

An experimental set-up for Raman experiments is shown in Fig. V.13, which was used for concentration measurements of exhaust

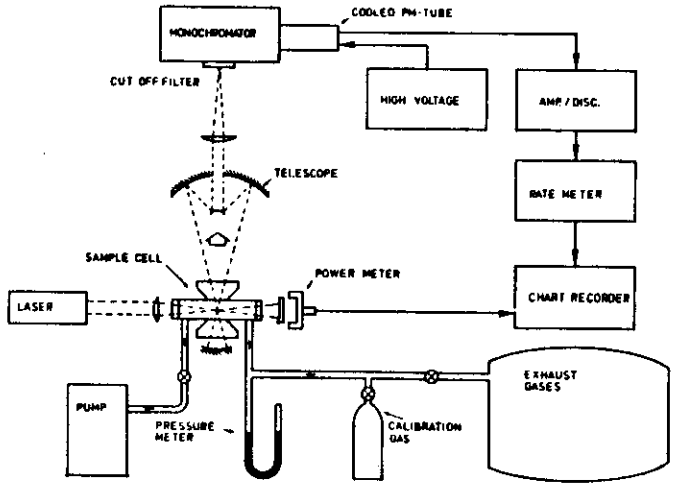

Figure V.13 . Experimental set-up for Raman experiments [b].

gases. Since, as already mentioned, the Raman effect is so weak, special efforts are often made to increase the signal strength. In Fig. V.13 this was achieved by placing the sample cell inside the laser cavity thereby increasing the laser intensity. A spherical mirror was also placed behind the cell in order to catch additional light. Similar intracavity enhancements of the Raman signals have been reported, e.g in [186-188], whereas multipass enhancement outside the laser cavity has been shown by Hill et al. [189-191]. When probing exhaust gases the Raman signals may be swamped in laser-induced fluorescence caused by particles. This problem was avoided in Paper 6 by using a simple filter system. More sophisticated fluorescence supression techniques are described by Setchell and Aeschliman [192-193]. In Fig. V.14 Raman spectra from gases sucked at two different

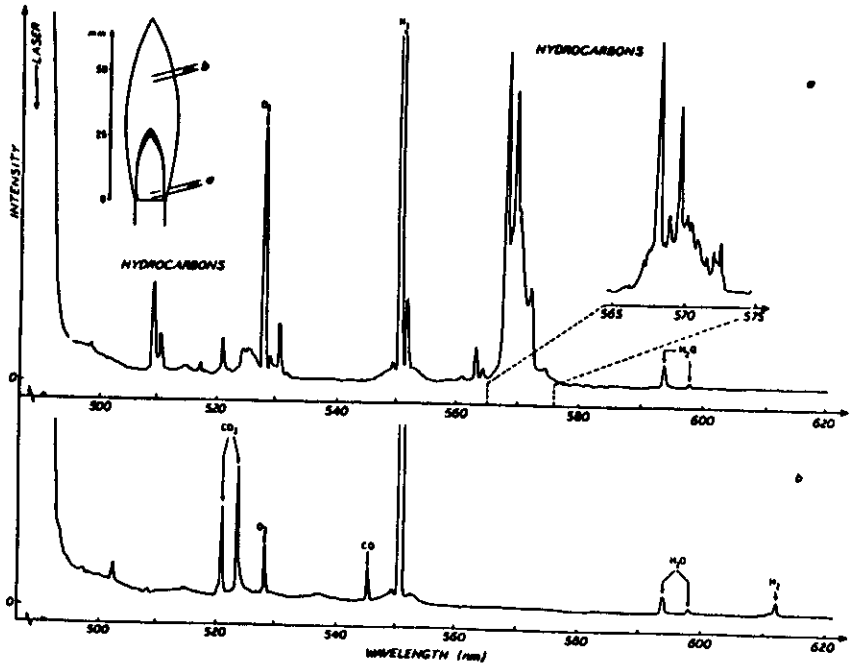

Figure V.14 . Raman spectra from two different positions in a flame [d].

positions in a propane Bunsen-burner flame are shown. It is illustrated how the fuel and oxygen are consumed and carbon-dioxide and carbonmonoxide are created. (The water peak is not representative since the gases were sucked through a water condensor). In order to examine the detectivity limit, calibration gases of 880 ppm NO and 1.6 % CO were examined. Resulting spectra are shown in Fig. V.15 a) and b). Recently Leipertz et

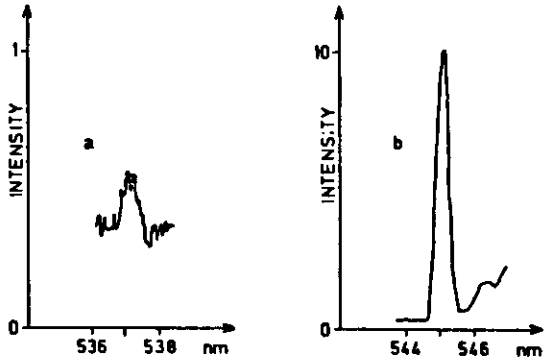

Figure V.15 . Raman spectra of a) 880 ppm NO and b) 1.6 % CO. [b]

al.[194] have measured gas concentrations down to 100 ppm using a ruby laser, whereas Hargis [195,196] used a KrF-laser to detect below 5 ppm of CH_4. However, as pointed out by Hargis, special care has to be taken using this high power UV beam, due to multiphoton photodissociation.

In order to measure number densities it is important to know the relative Raman cross-sections of gases. Table V.3 shows the Raman frequencies and corresponding cross-sections for gases of importance in combustion phenomena. The Raman cross-sections are normalized to N_2 where $\frac{d\sigma(N_2)}{d\Omega}$ is set to 0.46×10^{-30}

Table V.3 Different molecules of interest in combustion chemistry, and the corresponding Raman shifts and cross-sections.

Molecule	Ramanshift (cm^{-1})	$d\sigma/d\Omega(5320)$
N_2	2331	1
$NO_2(\nu_2)$	754	7.9
SF_6	775	3.9
$C_6H_6(\nu_2)$	991	12.2
O_3	1103	2.6
$SO_2(\nu_1)$	1151	5.4
$N_2O(\nu_1)$	1285	2.1
$CO_2(2\nu_2)$	1286	0.98
C_3H_6	1297	
$NO_2(\nu_1)$	1320	16.0
$CO_2(\nu_1)$	1388	1.3
C_3H_8	1451	
O_2	1556	1.41
$C_2H_4(\nu_2)$	1623	1.65
C_2	1832	
NO	1876	0.43
C_2H_2	1973	4.74
CN	2045	
CO	2145	1.04
N_2O	2224	0.5
$H_2S(\nu_1)$	2611	5.22
CH	2633	
CH_2O	2766	
HCl	2886	3.2
$CH_4(\nu_1)$	2914	5.65
D_2	2986	2.56
$CH_4(\nu_3)$	3017	3.70
$C_2H_4(\nu_1)$	3020	4.13
NH	3048	
$C_6H_6(\nu_1)$	3070	8.0
HCN	3311	
$NH_3(\nu_1)$	3334	2.83
H_2O	3652	1.96
OH	3665	
HF	3962	1.26
H_2	4160	1.85

cm^2/sr [87]. The values in Table V.3 are from Refs. [87,197], and calculated to an excitation wavelength of 5320 Å.

Raman spectroscopy is very useful for concentration measurements and has been used in investigations of jets [198,199], gas mixing phenomena [200,201], both laminar [202,203] and turbulent flames [204-206] and in internal-combustion engines [207-209].

V.2.3 Temperature Measurements

Raman scattering is very well suited for temperature measurements of combustion gases since the intensity of a Raman line is directly proportional to the Boltzmann factor. There are many ways of performing a temperature measurement using Raman spectroscopy, utilizing both rotational and vibrational Raman scattering.

If first pure rotational Raman scattering is considered, the intensity of line J is given by [183]

$$I_J \sim N_J(\nu \pm \nu_R)^4 \cdot S_J \qquad (23)$$

where S_J is the line strength. Using the selection rules for Raman transitions, and the expressions for S_J given in Ref. [1], the Stokes and anti-Stokes rotational intensities can be expressed as

$$I_S(J) = \frac{C\ N\ g_J (J+1)(J+2)[\nu - 4B(J+3/2)]^4}{(2J+3)Q_r} \exp[-BJ(J+1)\,hc/kT] \qquad (24)$$

$$I_{AS}(J) = \frac{C\ N\ g_J (J-1)\,J\,[\nu + 4B(J+3/2)]^4}{(2J-1)Q_r} \exp[-BJ(J+1)\,hc/kT] \qquad (25)$$

where C is a constant including the laser intensity, collection efficiency etc., and g_J is the nuclear-spin function. The temperature can be estimated by measuring the

intensities of two rotational lines with quantum numbers J and J'. The temperature using the Stokes branch is thus given by

$$T_S = \frac{[J'(J'+1) - J(J-1)]\ \frac{hcB}{k}}{\ln\left[\left(\frac{I_S(J)}{I_S(J')}\right)\frac{g_{J'}}{g_J}\left[\frac{\frac{(J'+1)(J'+2)}{(2J'+3)}}{\frac{(J+1)(J+2)}{(2J+3)}}\right]\left(\frac{\nu - 4B(J'+3/2)}{\nu - 4B(J+3/2)}\right)^4\right]} \qquad (26)$$

with a similar expression for T_{AS}. Fig. V.16 shows how the temperature can be estimated through plotting $I_S(J)/I_S(J')$ for J=6, J'=18 and J=4, J'=20 as a function of temperature for

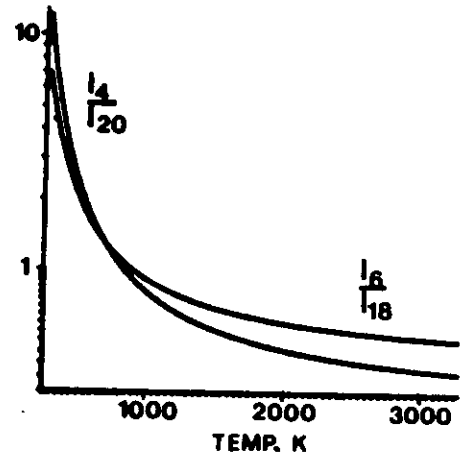

Figure V.16 . The temperature dependence of the ratio of two rotational Raman-lines intensities.

the N_2 molecules. Alternatively, the rotational temperature can be estimated through rearrangement of Eq. (24) and a straight-line plotting procedure, where the temperature is deduced from the slope of the line.

When using rotational Raman scattering for temperature

measurements, it is important to use a monochromator with high background rejection, preferrably a double monochromator or a Fabry-Perot interferometer.

Drake et al. [210-212] have used rotational Raman scattering for flame temperature measurements, whereas Hickman et al. [213] measured the gas temperature in an intracavity cell and Barrett et al. [214] measured the temperature in an electrical discharge using a F-P interferometer and the pure rotational Raman effect. Recently, spontaneous Raman scattering has been used for detection of oxygen atoms in a H_2/O_2 flame [215]. The atom lines appear at 158 and 227 cm^{-1}, and may be partially masked by rotational lines from O_2, if the resolution is not high enough.

Although rotational Raman scattering has been successfully applied for temperature measurements in combustion zones, most work has been carried out using vibrational transitions. Pioneering work in temperature measurements was carried out by Lapp and Penney et al. in the early seventies [216-219]. There are four common methods of determining temperature from vibrational Raman scattering. The most straight-forward technique is to compare the intensity of the integrated Stokes and anti-Stokes intensities. This ratio is given by [220]

$$\frac{I_S}{I_{AS}} = \left(\frac{\nu-\nu_R}{\nu+\nu_R}\right)^4 \exp\left[\frac{hc\nu_R}{kT}\right] \qquad (27)$$

This ratio as a function of temperature for three different molecules is shown in Fig. V.17. This technique for temperature measurements has been used by Widhopf et al. [221], and by Drake et al. [222] for determinations of probability density functions (pdf's) of temperatures in turbulent diffusion flames. One drawback with the Stokes to anti-Stokes approach is that the bands are separated by a large wave number interval, ~4660 cm^{-1} for N_2 , which means that proper corrections for differences in sensitivity, background and absorption have to be made. This problem is avoided in the other three techniques, that are

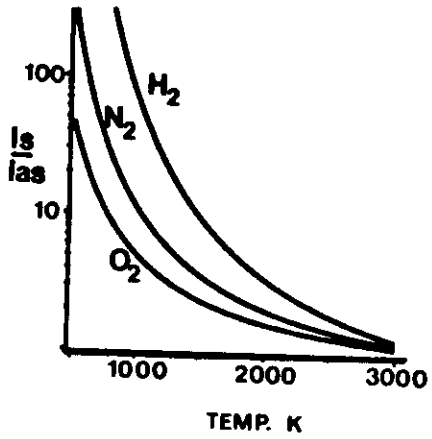

Figure V.17 . The Stokes to anti-Stokes ratio as a function of temperature for H_2,N_2 and O_2.

based on investigations of the Q-branch of e.g. N_2. At high temperature the excited states v=1, v=2 start to be populated. Due to the molecular anharmonicity these bands are frequency-shifted and give rise to a characteristic sawtooth-like spectrum A Raman spectrum of N_2 from a H_2/air flame, with a fundamental band (v=0 → v=1) and the "hot band" (v=1→ v=2) is shown in Fig. V.18. The separation between these bands is only about 30 cm^{-1} for N_2.

The intensity for an individual line in the vibrational Stokes Q-branch ($\Delta J=0$, $\Delta v=1$) is given by [216]

$$I(v,J) \sim \frac{g_J(2J+1)(v+1)(\nu-\nu_R)^4}{Q_r Q_v} \exp\left[-\frac{hc}{kT} G(v,J)\right] \qquad (28)$$

For the anti-Stokes signal ($\Delta v=-1$), the vibrational amplitude factor v+1 is replaced by the factor v [223]. Experimentally, the observed intensity is due to several individual lines modified

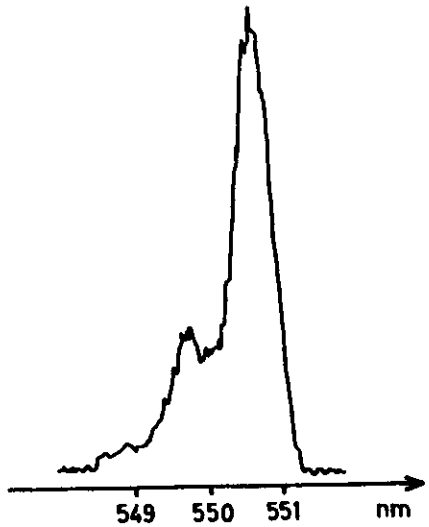

Figure V.18 . Raman spectrum from N_2 molecules in a flame. [b]

by an instrument function g(ν)

$$I_{obs} = \sum_{v,J} I(v,J)\, g(\nu) \qquad (29)$$

One technique is based on comparing the maximum intensity of the fundamental band to the maximum intensity of the first hot band, as used by Stricker [224] and Stephenson et al. [225]. The second technique, frequently called the Band Area Method [219], compares the total intensity of the hot band to that of the fundamental band. In the third method the complete contour of a band is calculated and fitted to an experimental spectrum. This technique has been extensively used see e.g. [226-229].

So far, the discussion has been limited to the analysis of diatomic molecules and preferrably N_2. The reason for this is obvious, the molecular spectra become much more complicated as the molecule grows. As can be seen from Fig. V.19 the Raman

spectrum of H_2O from an H_2/air flame is much broader and more complex than the N_2 spectrum in Fig. V.18. Nevertheless, theoretical spectra of H_2O [230,231] and CO_2 [231,232] have been calculated which show good agreement with experimental ones, and have consequently been used for temperature and concentration measurements in flames.

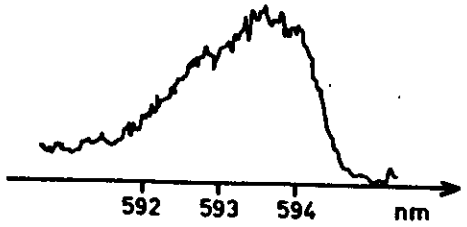

Figure V.19 . The Raman spectrum of H_2O molecules in a flame [b].

In the previous section it was described how intermediate radicals could be visualized using an optical multichannel analyzer. Such experiments using Raman techniques were already outlined in 1974 by Hartley [233] , who called it Ramanography. This technique was also used by Webber et al. [234] in experiments on a CH_4-jet. The application of multichannel detectors for Raman scattering in combustion diagnostics has also been illustrated in Ref. [235].

V.3 Coherent anti-Stokes Raman Scattering

Coherent anti-Stokes Raman scattering or CARS is an optical nonlinear effect that was discovered by Maker and Terhune in 1965 [236]. During the seventies, applications were found in several areas, such as chemistry, biology and physics . For reviews see Refs. [237-239]. The application of CARS in combustion diagnostics was first realized by Taran and coworkers [240-242],

and now several review articles describing CARS as a diagnostic tool in combustion research have appeared [243-246]. The CARS theory and the different experimental approaches are discussed in Paper 8 and the field will here be briefly summarized.

V.3.1 Theory

The CARS effect may be described as an interaction of two photons from one laser beam at frequency ω_p, and one photon from a laser beam at frequency ω_S through the third-order nonlinear susceptibility $\chi^{(3)}$ to generate an anti-Stokes photon at $\omega_{AS}=2\omega_p-\omega_S$. The CARS generation can be described both classically using Maxwell's equations or quantum-mechanically utilizing the density matrix theory, as described by St. Peters [247,248], DeWitt et al. [249] and by Druet et al. [250,251].

It can be shown that the CARS intensity I_{AS} at frequency ω_{AS} may be written [87]

$$I_{AS} = \left[\frac{4\pi^2 \omega_{AS}}{c^2}\right]^2 I_p^{\,2} I_S^{\,2} |\chi|^2 z^2 \qquad (30)$$

where I_p and I_S are the laser intensities of the pump and Stokes beam, respectively, and z is the path length from which the CARS signal is generated. Following the presentation in [87], the third-order susceptibility can be divided into a resonant and a non-resonant part

$$\chi = \chi_R + \chi_{NR} \qquad (31)$$

where the non-resonant part χ_{NR}, arises from electronic transitions and remote Raman transitions, and χ_R consists of one real and one imaginary part. For a Raman transition j we thus have

$$\chi_R = \chi' + i\chi'' = \frac{2c^4}{\hbar\omega_S^{\,4}} N\Delta_j b_j \left(\frac{d\sigma}{d\Omega}\right)_j \frac{\omega_j}{\omega_j^{\,2}-(\omega_p-\omega_S)^2-i\Gamma_j(\omega_p-\omega_S)} \qquad (32)$$

In this equation $N\Delta_j$ is the population difference between the initial and final states, b_j is the line strength factor, $d\sigma/d\Omega$ is the Raman cross-section for the molecular species and Γ_j is the Raman linewidth. Examining Eqs. (30)-(32) several differences between CARS and spontaneous Raman scattering can be seen. Firstly, the CARS signal is highly nonlinear in both number density, laser intensity and Raman cross-section, whereas ordinary Raman scattering has a linear dependence of these factors. Secondly, the CARS process involves the population difference between the levels involved in the process, which means that $N\Delta_J$ is equal to N for low temperature and 0 for infinite temperature. Finally the CARS process also involves the Raman linewidth Γ_j. From Eqs. (31) and (32) it can be seen

$$|\chi|^2 = \chi'^2 + \chi''^2 + 2\chi'\chi_{NR} + \chi_{NR}^{\,2} \qquad (33)$$

Since χ' has a dispersive behaviour whereas χ'' has lineshape behaviour and χ_{NR} is a constant, a CARS spectrum has a complex lineshape depending on the magnitude of χ_{NR}. This can be explained according to Fig. V.20, which shows the behaviour for a weak and a strong line. If χ_{NR} is small, the resulting CARS lineshape is given by $\chi'^2 + \chi''^2$ and does not reveal any unusual spectral features as shown in Fig. V.20a. However, if χ_{NR} is large in Eq.(33), the resulting CARS lineshape is given by

$$|\chi|^2 \simeq \chi_{NR}^{\,2} + 2\chi'\chi_{NR} \qquad (34)$$

which means that the CARS resonance appears as a modulation of a background as shown in Fig. V.20b. The occurence of χ_{NR} is limiting the possibility to detect small number densities, and several approaches have been suggested to avoid this problem, which will be described later. When several resonances are present, as in a rotational-vibrational molecular band, the resulting CARS spectrum is further complicated through strong interactions of neighbouring resonances and the background.

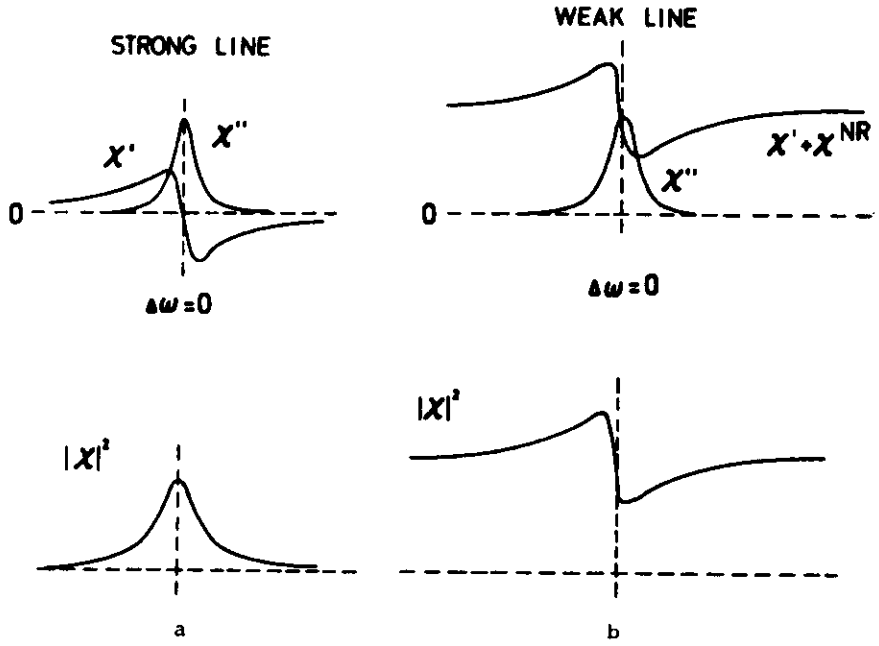

Figure V.20 . a) The CARS lineshape for strong line b) The CARS lineshape for a weak line.

The origin for the CARS process may be schematically described by an energy level diagram as shown in Fig. V.21, where two photons at ω_p and ω_S beat the Raman vibration ω_R, which then is coupled to a second ω_p photon and give rise to a anti-Stokes photon at $(\omega_p-\omega_S)+\omega_p=\omega_{AS}$. In order to achieve high efficiency in the CARS process it is important to fulfil the phase-matching condition, which is illustrated to the right in Fig. V.21. The simplest type of phase-matching is the collirear approach (at the top), but since the spatial resolution normally is too low with this approach. The BOXCARS approach, shown in the middle, was introduced by Eckbreth [252]. However, when probing Raman transitions with small shifts, also this technique may be troublesome. This problem was solved by the introduction

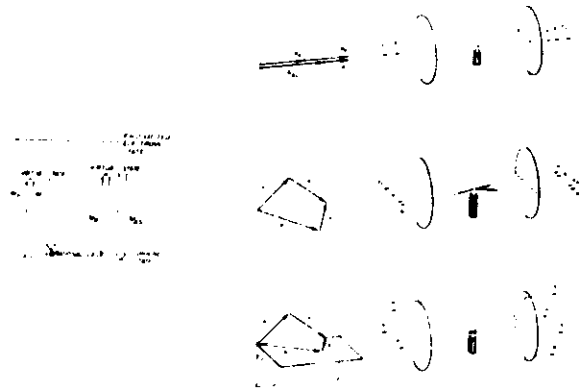

Figure V.21 .The energy level diagram describing the CARS process (to the left), and different phase-matching conditions (to the right)

of folded BOXCARS (at the bottom), where all the input laser beams are spatially separated [253-255]. Recent calculations by Greenhalgh [256] show that for a half crossing angle of the pump beams of less than 20 degrees, there is no significant loss in the CARS intensity in going from planar BOXCARS to folded BOXCARS.

V.3.2 Experiments

As has been pointed out the first combustion measurements using CARS were performed by Taran et al. In these early experiments on hydrogen in flames, the Stokes beam was produced by stimulated Raman scattering in a high pressure H_2 cell. In this way the hydrogen contents were mapped out in a hydrocarbon flame.

Up till 1976 all CARS spectra were recorded through scanning the frequency of the Stokes beam ω_S, whereas the pump beam was held fixed at ω_F. In this way the applicability of CARS was limited to stationary media. However, in 1976 Roh et al. [257] showed how

a complete CARS spectrum could be captured in a single laser pulse, using a broadband dye laser.

As was described in the previous section, a CARS spectrum is quite complex and for quantitative measurements of e.g. temperatures it is almost necessary to have a computer code for generating theoretical CARS spectra. Such computer codes have been realized in several laboratories e.g. [258-261]. An example of a computer generated CARS spectrum for N_2 at 2000 K and a resolution of 0.5 cm^{-1} is shown in Fig. V.22, which was generated with a code, that was kindly put to our disposal by R.J.Ball.

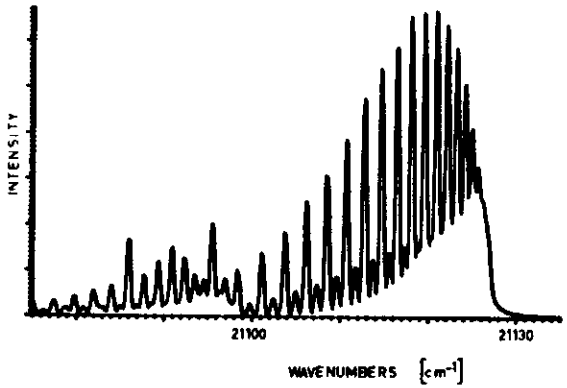

Figure V.22 . Theoretical CARS spectrum for N_2 at 2000 K , and a resolution of 0.5 cm^{-1}

In the last ten years several papers describing CARS measurement in flames [262-266], sooty flames [267,268], combustors [269-271] and internal combustion engines [272-274] have been reported, and recently a detailed comparison between CARS and thermocouple temperature measurements was published by Farrow et al. [275]. An example of broadband CARS spectra in a flame is illustrated in Fig. V.23, which shows BOXCARS spectra of O_2 at three different positions in the flame. This figure clearly illustrates the temperature effect on the spectra. The spatial resolution in this kind of experiment can be measured through translating a micro-

Figure V.23 . CARS spectrum of O_2 at different positions in a flame, captured using a diode array detector [276].

scope slide through the focal region, and recording the CARS signal from the slide as it is moved. Such a recording is shown in Fig. V.24, where the square root of the intensity is displayed

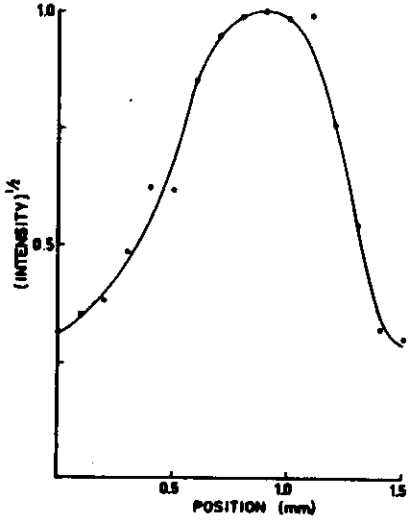

Figure V.24 Illustration of the spatial resolution of the CARS signal [277].

as a function of distance. Fig. V.24 indicates a spatial resolution of about 1 mm, which could be increased or decreased by either changing the focusing lens or the angle between the laser beams.

For the same reason as in Raman spectroscopy, preferrably the spectra of diatomic molecules have been investigated for temperature measurements. However, Hall et al. [263,278] have constructed a computer code for CO_2 and H_2O which yields very good agreement with experimental spectra. As can be seen from Fig. V.25, which shows a CO_2 broadband BOXCARS spectrum from a CO/air flame, the spectrum does not show a rotational smearing of

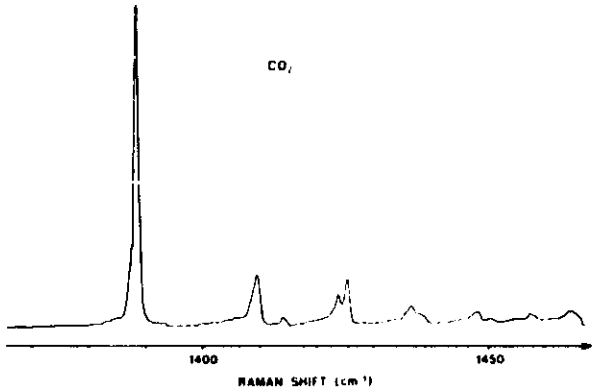

Figure V.25 CARS spectrum of CO_2 molecules in a CO/air flame [279].

the vibrational lines, due to a very small vibration-rotation interaction in this molecule [280], and the different peaks correspond to transitions between different vibration modes. (We recall from Chapter II that CO_2 has 3 x 3 - 5 = 4 different vibration modes). The CARS spectra shown in Figs. V.23 and 25 were captured using a diode array detector and as described in Papers 7 and 8 ,this type of detector is one-dimensional, which means that it is difficult to correct for the spectral nonreproducibility of the broadband dye laser pulses. However, using a double-slit in the monochromator entrance plane, and utilizing two parts of the diode array, proper corrections may be performed. We have made preliminary double-slit experiments, where a Na calibration lamp was used. The result is shown in Fig. V.26a and b. In Fig. V.26 a) the resulting Na doublet using one slit in a 1 m Jobin-Yvon HR 1000 is shown, whereas the double slit spectrum is shown in Fig. V.26 b).

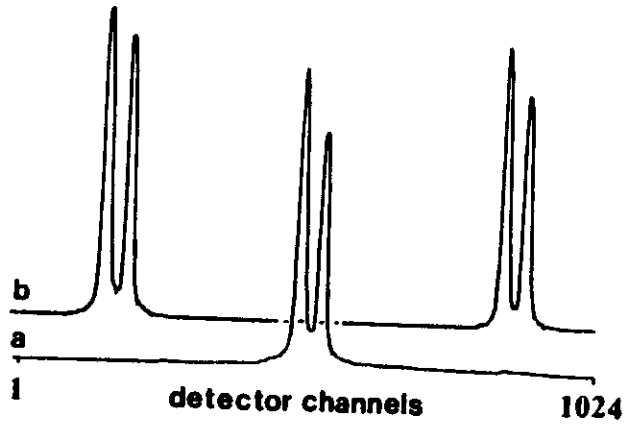

Figure V.26 . a) The Na spectrum as when using a single slit b) The spectrum when using a double-slit arrangement [281].

Measurements of the vibrational and rotational populations in sparks and electrical discharges represent a field for which the CARS technique looks very promising. Already in 1976 Nibler et al. [282] used CARS in this context to measure the vibrational population of D_2 in an electrical discharge, and in 1978 Smirnov et al. [283] used a high-resolution set-up to measure the vibrational, as well as rotational distribution in a discharge. Recently Pealat et al. [284] studied a hydrogen plasma whereas Dreier et al. [285] have used CARS to measure the vibrational population of N_2 in a microwave-excited N_2-CO-He mixture. Typical CARS spectra of N_2 at different positions in a DC

discharge are shown in Fig. V.27. These spectra, which all are

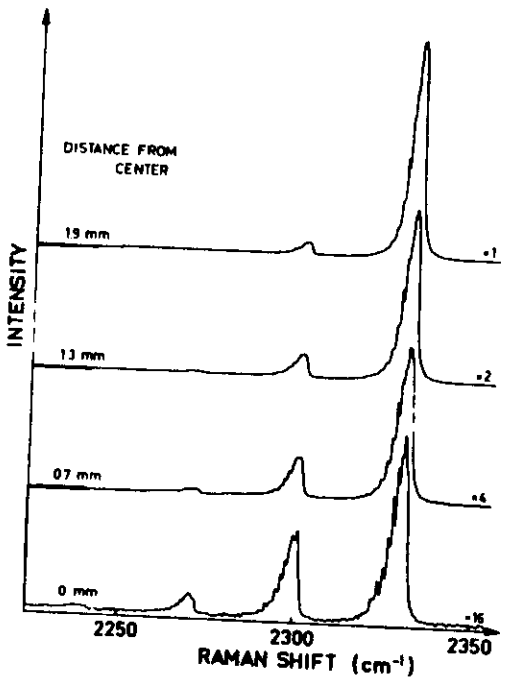

Figure V.27 . BOXCARS spectra of N_2 at different positions in a DC discharge [277]

broadband BOXCARS spectra, show a considerable departure from thermal equilibrium with a high vibrational temperature (~3000 K) and a low rotational temperature (~400 K).

As has been described, the presence of χ_{NR}, the non-resonant contribution to the third-order nonlinear susceptibility, is a complication when low number densities are to be measured, and several approaches have been suggested for avoiding this problem.

a) Background cancellation can be achieved through introducing a second tunable laser at ω_p' . When $\omega_p - \omega_S$ is tuned to a

resonance, e.g. in N_2 and $\omega_p' - \omega_S$ is tuned to a resonance of a minor constituent, the background may be supressed by a negative contribution from the first resonance. Lynch et al. have stated, that χ_{NR} could be supressed by at least one order of magnitude [286].

b) Supression of χ_{NR} can also be achieved through taking advantage of the different temporal behaviour of χ_{NR} and χ_R This technique requires picosecond laser pulses and has been shown to reduce the background by two orders of magnitude [287].

c) A large increase in χ_R can be achieved if the laser sources are tuned to an electronic resonance of the molecule. Resonant CARS has been shown in e.g. NO_2 by Guthals et al. [288], in I_2 vapour by Attal et al. [289], and was theoretically investigated by e.g. Druet et al. [251,290]. Recently, Taran and co-workers [291,292] used resonance CARS to measure C_2 in a microwave discharge and in an oxy-acetylene flame at a number density of 5×10^{11} cm^{-3} and 10^{13} cm^{-3}, respectively. From these experiments a detection sensitivity of about 10^{10} cm^{-3} was deduced, which is about 10^6 times lower than the detectivity limit for e.g. CO at flame temperatures.

d) The most promising technique for background rejection is maybe polarization CARS [293-296], which utilizes the different tensor properties of χ_{NR} and χ_R. Thus, it was shown that the background could be rejected when the input laser beams were polarized at a certain angle to each other, and detection of the CARS beam followed at another specific angle. Rahn et al. [293] have shown an increase of signal-to-noise of over 200 when using polarization CARS instead of normal CARS in detecting CO in a flame. Unfortunately, the polarization variant of CARS results in a large reduction in signal strength and Eckbreth et al. have made a detailed investigation of how the detectivity can be increased using polarization CARS in detection of minor constituents in flames [296].

Another variant of CARS is rotational CARS, which is described in

Paper 7. This technique has a great potential since several species may be detected simultaneously using a broad-band dye laser. Further, low temperatures can be measured with high accuracy. Rotational CARS experiments have been reported in e.g. [297-299].

When using CARS with high power laser beams it is important to avoid saturation effects. According to Taran et al. [300] there are two potential perturbations. The first is stimulated Raman gain where the Stokes beam is amplified due to stimulated Raman scattering. However, this effect is in general weak. The other effect, which changes the population difference factor through vibrational saturation may be severe and thus makes temperature measurements impossible.

Another effect that limits the intensity of the laser beam, not only in CARS but also in Raman and laser-induced fluorescence experiments, is optical breakdown, which means that the medium becomes fully ionized and thus not available for diagnostic purposes. The laser-induced breakdown effect is treated in [301] where wavelength and pressure dependence etc. on the breakdown threshold is discussed.

V.4 Other Laser Diagnostic Techniques

This presentation of laser techniques in combustion diagnostics has been focused on laser-induced fluorescence, Raman scattering and CARS, since these techniques have been the ones that are most used. However, there are several other techniques which under certain circumstances may be very valuable diagnostic tools. In this section some of these techniques will be briefly described.

Absorption. Traditional absorption measurements of gas concentrations and temperatures have been used for a long time. Eg. Chou et al. [302] used this technique for measurements of concentration flame profiles of OH, NH and NH_2, whereas Schoenung et al. [303] measured CO concentrations and temperatures in a flame

using a tunable diode laser around 4.7 μm. In order to increase the absorption, Harris et al. used intracavity absorption to measure atomic oxygen [304] in a discharge flow, and C_2 in an oxy-acetylene flame [305].

The great drawback with the absorption technique is that it is a line-of-sight technique. Thus the resolution is very poor. Recent experiments have demonstrated how to get space resolved absorption measurement, through saturated absorption [306], optical Stark modulation [307] and optical Stark shifting [308].

Optogalvanic detection. The optogalvanic technique is based upon measurement of the current caused by laser ionization of molecules or atoms. The technique has been reviewed by Smyth et al. [309], and recently Goldsmith [310,311] used a multiphoton optogalvanic approach to detect oxygen and hydrogen atoms in flames. The disadvantage with the optogalvanic technique is that the electrodes and the applied voltage may disturb the flow conditions.

Photoacoustic techniques. In the photoacoustic technique the gas is illuminated with resonant laser light. The excited molecules can loose their energy radiatively or by collisions. The collisions appear as an increase in the translation energy of the molecules. At constant temperature this results in a pressure increase, which can be detected. This technique has been used by Tennel et al. [312] for minor constituent measurements in flames. The same technique was used by West et al. [313] in a pure rotational stimulated Raman experiment. A variant of the photoacoustic technique was proposed by Zapka et al. [314] in which a strong laser pulse is producing a breakdown in the flame, and by measuring the acoustic pulse propagation by two He-Ne laser beams the flame temperature could be measured.

Raman gain/loss spectroscopy. In Raman gain/loss experiments a strong pump beam at frequency ω_p produces a gain at the Stokes frequency; alternatively, a loss at the anti-Stokes frequency. By using a probe laser this gain/loss can be detected. Both these effects originate from the imaginary part of the third-order

nonlinear susceptibility. The effects have been observed both with pulsed sources [315], CW sources [316], and with a combination of pulsed and CW laser beams [317]. The applicability to flames was realized by Owyoung and Rahn in 1979 [318], and recently Rahn reported time-resolved measurements [319]. A polarization variant of this technique is the Raman-Induced Kerr Effect (RIKES), discovered in 1976 [320].

Elastic Scattering. This field, which is rather large includes Rayleigh scattering for temperature measurements [321,322], flow visualization [323], and density measurements [324], and Mie scattering for particle-size [325], and flow-velocity measurements [326].

67. Y.R. Shen, Reviews of Modern Physics, 48, 1 (1976).

68. M.R. Topp, Appl. Spectr. Rev. 14, 1 (1978).

69. R.W. Terhune and P.D. Maker, "Nonlinear optics" pp 295 in in "Lasers" Ed. A.K. Levine, Marcel Dekker, N.Y. 1968.

70. G.C. Bjorkholm and R.H. Storz, IEEE J. of Quant. Electr. 15, 228 (1979).

71. B. Nilsson and P. Norrman, Lund Reports on Atomic Physics, LRAP-10, 1981.

72. J. Paisner and S. Hargrove, Energy and Techn. Rev. (March 1979).

73. Y. Talmi, Anal. Chem. 47, 658 A (1975).

74. Y. Talmi, Anal. Chem. 47, 699 A (1975).

75. Y. Talmi, American Laboratory, March 1978, p 79.

76. J.L. Chao, Appl. Spectr. 35, 281 (1981).

77. G. Horlick and E.G. Codding, Anal. Chem. 45 1490 (1973).

78. E.H. Snow, Research/Development, p 18 (April 1976).

79. Tracor Northern Operation Manuale for DARSS Modules,

80. M. Aldén, C.M. Penney and S. Warshaw, Unpublished.

81. Laser Focus, p 20 (March 1982).

82. M. Lapp and C.M. Penney, Eds., "Laser Raman Gas Diagnostics", Plenum Press, 1974.

83. B.T. Zinn, Ed., "Experimental Diagnostics in Gas Phase Combustion Systems", Vol. 53, Progress in Astronautics and Aeronautics, Jan. 1976.

84. R. Goulard, Ed., "Combustion Measurements, Modern Techniques and Instrumentation", Academic Press, 1976.

85. H. Schlossberg, Ed., "Laser Spectroscopy - Applications & Techniques", Proceedings of the Society of Photo-Optical Instrumentation Engineers, Vol. 158 (1978).

86. D.R. Crosley, Ed., "Laser Probes for Combustion Chemistry", ACS Symposium Series 134, American Chemical Society, Washington 1980.

87. A.C. Eckbreth, P.A. Bonczyk and J.P. Verdieck, Progress in Energy and Combustion Science 5, 253 (1979).

88. J.H. Bechtel and A.R. Chraplyvy, Proc. of the IEEE 70, 658 (1982).

89. C.P. Wang, Comb. Sci. Techn. 13, 211 (1976).

90. K. Schofield and M. Steinberg, Opt. Eng. 20, 501 (1981).

91. D.R. Crosley, J. Chem. Ed. 59, 446 (1982).

92. M. Aldén and H. Edner, Unpublished.

93. K.H. Becker, D. Haaks and T. Tatarczyk, Z. Naturforsch. 27a, 1520 (1972).

94. C.C. Wang and L.I. Davis Jr., Appl. Phys. Lett. 25, 34 (1974).

95. D. Stepowski and M.J. Cottereau, Appl. Opt. 18, 354 (1979).

96. J.H. Bechtel and R.E. Teets, Appl. Opt. 18, 4138 (1979).

97. B.T. Ahn, G.J. Bastiaans and F. Albahadily, Appl. Spectr. 36, 106 (1982).

98. R.P. Lucht, D.W. Sweeney and N.M. Laurendeau, Paper presented at the 1982 Spring Meeting, Western States Section/The Combustion Institute.

99. M.J. Cottereau and D. Stepowski, p 131 in Ref. [86].

100. R.P. Lucht, D.W. Sweeney and N.M. Laurendeau, p 145 in Ref. [86].

101. C. Morley, Comb. and Flame 47, 67 (1982).

102. K. Fujiwara, N. Omenetto, J.B. Bradshaw, J.N. Bower, S. Nikdel and J.D. Winefordner, Spectrochim. Acta 34B, 317 (1979).

103. W.R. Anderson, L.J. Decker and A.J. Kotlar, Comb. and Flame 48, 179 (1982).

104. C. Chan and J.W. Daily, Appl. Opt. 19, 1357 (1980).

105. D.G. Jones and J.C. Mackie, Comb. and Flame 27, 143 (1976).

106. A.P. Baronavski and J.R. McDonald, J. Chem. Phys. 66, 3300 (1977).

107. A.P. Baronovski and J.R. McDonald , Appl. Opt. 16, 1897 (1977).

108. M. Mailänder, J. Appl. Phys. 49, 1256 (1978).

109. M.B. Blackburn, J.M. Mermet and J.D. Winefordner, Spectrochim. Acta 34A, 847 (1978).

110. V.I. Lokhman, D.O. Ogurok, N.V. Chekalin and A.N. Shibanov, Opt. Spectrosc. 46, 426 (1979).

111. K.H. Becker, D. Haaks and T. Tatarczyk, Z. Naturforsch. 29a, 829 (1974).

112. R.H. Barnes, C.E. Moeller, J.F. Kircher and C.M. Verber, Appl. Opt. 12, 2531 (1973).

113. P.A. Bonczyk and J.A. Shirley, Comb. and Flame 34, 253 (1979).

114. R.J. Cattolica, D. Stepowski, D. Puechberty and M. Cottereau, Sandia Report, Sand 82-8615, 1982.

115. A.C. Eckbreth, P.A. Bonczyk and J.F. Verdieck, United Technology Research Center Technical Report EPA-600/7-80-091, 1980.

116. C. Morley, Proc. 18th Symp. on Combustion, The Combustion Institute 1981, p 23.

117. D.R. Grieser and R.H. Barnes, Appl. Opt. 19, 741 (1980).

118. B.J. Sullivan, G.P. Smith, D.R. Crosley and G. Black, Paper presented at The Eastern Section of the Combustion Institute, Pittsburg, Oct. 1981.

119. W.R. Anderson, J.A. Vanderhoff, A.J. Kotlar, M.A. Dewilde and R.A. Beyer, J. Chem. Phys. 77,1677 (1982).

120. R.H. Barnes and J.F. Kircher, Appl. Opt. 17, 1099 (1978).

121. L. Pasternack, H.H. Nelson, J.R. McDonald, J. Chem. Ed. 59, 456 (1982).

122. K.H. Becker, U. Schurath and T. Tatarczyk, Appl. Opt. 14, 310 (1975).

124. J.B. Halpern, G. Hancock, M. Lenzi and K.H. Welge, J. Chem. Phys. 63, 4808 (1975).

125. C.H. Muller III, K. Schofield and M. Steinberg, p 103 in Ref. [86].

126. J.A. Gelbwachs, C.F. Klein and J.E. Wessel, Appl. Phys. Lett. 30, 489 (1977).

127. J.H. Brophy, J.A. Silver and J.L. Kinsey, Chem. Phys. Lett. 28, 418 (1974).

128. E.E. Piepmeier, Spectrochim. Acta 27B, 431 (1972).

129. J.W. Daily, Appl. Opt. 16, 568 (1977).

130. N. Omenetto, L.P. Hart, P. Benetti and J.D. Winefordner, Spectrochim. Acta 28B, 301 (1973).

131. J.W. Daily and C. Chan, Comb. and Flame 33, 47 (1978).

132. R.K. Lengel and D.R. Crosley, J. Chem. Phys. 67, 2085 (1977).

133. G.P. Smith, D.R. Crosley and L.W. Davis, Paper presented at Eastern States, Meeting of the Combustion Institute, Atlanta 1979.

134. D. Stepowski and M.J. Cottereau, J. Chem. Phys. 74, 6674 (1981).

135. R.K. Lengel and D.R. Crosley, J. Chem. Phys. 68, 5309 (1978).

136. D.R. Crosley, Opt. Eng. 20, 511 (1981).

137. R.P. Lucht and N.M. Laurendeau, Appl. Opt. 18, 856 (1979).

138. J.O. Berg and W.L. Shackleford, Appl. Opt. 18, 2093 (1979).

139. J.W. Daily, p 61 in Ref. [86].

140. A.J. Kotlar, A. Gelb and D.R. Crosley, p 137 in Ref. [86].

141. J.F. Verdieck and P.A. Bonczyk, 18th Symposium on Combustion, The Combustion Institute, 1981, p 1559.

142. C.M. Muller III, K. Schofield and M. Steinberg, J. Chem. Phys. 72, 6620 (1980).

143. J.W. Daily, Appl. Opt. 17, 225 (1978).

144. R.A. Van Calcar, M.J.M. Van de Ven, B.K. Van Uitert, K.J. Biewenga, Tj. Hollander and C.Th.J. Alkemade, J. Quant. Spectr. Rad. Transf. 21, 11 (1979).

145. D. Stepowski and M.J. Cottereau, Comb. and Flame, 40, 55 (1981).

146. J.W. Daily, Appl. Opt. 17, 1610 (1978).

147. J.H. Bechtel, Appl. Opt. 18, 2100 (1979).

148. W.R. Anderson, L.J. Decker and A.J. Kotlar, Comb. and Flame 48, 163 (1982).

149. D.R. Crosley and G.P. Smith, Comb. and Flame 44, 27 (1982).

150. R. Cattolica, Appl. Opt. 20, 1156 (1981).

151. R.P. Lucht, N.M. Laurendeau and D.W. Sweeney, Appl. Opt. 21, 3729 (1982).

152. C. Chan and J.W. Daily, Appl. Opt. 19, 1963 (1980).

153. D.R. Crosley and G.P. Smith, Appl. Opt. 19, 517 (1980).

154. R.M. Kowalik and C.H. Kruger, Comb. and Flame 34, 135 (1979).

155. G. Zizak and J.D. Winefordner, Comb. and Flame 44, 35 (1982).

156. J. Bradshaw, J. Bower, S. Weeks, K. Fujiwara, N. Omenetto, H. Haraguchi and J.D. Winefordner, NBS Special Publication 561, 1979.

157. H. Haraguchi, B. Smith, S. Weeks, D.J. Johnson and J.D. Winefordner, Appl. Opt. 31, 156 (1977).

158. R.G. Joklik and J.W. Daily, Appl. Opt. 21, 4158 (1982).

159. K. Fujiwara, N. Omenetto, J.B. Bradshaw, J.N. Bower and J.D. Winefordner, Appl. Spectr. 34, 85 (1980).

160. J.H. Miller, W.G. Mallard and K.C. Smyth, Comb. and Flame 47, 205 (1982).

161. F. Beretta, A. Cavaliere and A. D'Alessio, Comb. Sci. and Tech. 27, 113 (1982).

162. D.S. Coe and J.I. Steinfeld, p 159 in Ref. [86].

163. M. Aldén and B. Galle, to be published.

164. M.J. Dyer and D.R. Crosley, Opt. Lett. 7, 382 (1982).

165. M.J.Dyer and D.R. Crosley, Western States Section of the Combustion Institute Fall Meeting, Paper 82-66, 1982.

166. G. Kychakoff, R.D. Howe, R.K. Hanson and J.C. McDaniel, Appl. Opt. 21, 3225 (1982).

167. G. Kychakoff, K. Knapp, R.D. Howe and R.H. Hanson, Western States Section of the Combusiton Institute Fall Meeting. Paper 82-60, 1982.

168. J. Bokor, R.R. Freeman, J.C. White and R.H. Storz, Phys. Rev. A 24, 612 (1981).

169. W.K. Bischel, B.E. Perry and D.R. Crosley, Appl. Opt. 21, 1419 (1982).

170. C.H. Muller III, D.R. Eames and K.H. Burrell, Bull. Am. Phys. Soc. 26, 1031 (1981).

171. R.L. McKenzie and K.P. Gross, Appl. Opt. 20, 2153 (1981).

172. T. Ozaki, Y. Matsi and T. Ohsawa, J. Appl. Phys. 52, 2593 (1981).

173. S.V. Filseth, R. Wallenstein and H. Zacharias, Opt. Commun. 23, 231 (1977).

174. D.R. Crosley and G.P. Smith, to be published.

175. T.R. Gilson and P.J. Hendra, "Laser Raman Spectroscopy", John Wiley, 1970.

176. J. Loader, "Basic Laser Raman Spectroscopy", Heyden & Son Ltd., 1970.

177. M.C. Tobin, "Laser Raman Spectroscopy", Wiley-Interscience, 1971.

178. A. Anderson Ed., "The Raman Effect, Principles Vol 1 and Applications Vol 2", Marcel Dekker, New York, Vol 1, 1971, Vol 2, 1973.

179. J.A. Konigstein, "Introduction to the Theory of the Raman Effect, Reidel, Dordrecht, Holland, 1972.

180. D.A. Long, "Raman Spectroscopy", McGraw-Hill, 1977.

181. M. Lapp and C.M. Penney, "Raman Measurements on Flames", in Advances in Infrared and Raman Spectroscopy, R.J.H. Clark and R.E. Hester Eds., Heyden and Son, 1977, p 204.

182. M. Lapp and D.L. Hartley, Comb. Sci. Techn. 13, 199 (1976).

183. S. Lederman, Prog. Energy Comb. Sci. 3, 1 (1977).

184. R.E. Setchell, AIAA Jour. 18, 181 (1980).

185. A.C. Eckbreth, AIAA Paper 74-1144, AIAA/SAE 10th Propulsion Conf., Oct. 1974.

186. G.O. Neely and L.Y. Nelson and A.B. Harvey, Appl. Spectr. 26, 553 (1972).

187. R.S. Hickman and L. Liang, Appl. Spectr. 27, 425 (1973).

188. M. Hercher, W. Mueller, S. Klainer, R.F. Adamowicz, R.E. Meyers and S.E. Schwartz, Appl. Spectr. 32, 298 (1978).

189. R.A. Hill and D.L. Hartley, Appl. Opt. 13, 186 (1974).

190. R.A. Hill, C.W. Peterson, A.J. Mulac and D.R. Smith, J. Quant. Spectrosc. Rad. Transf. 16, 953 (1976).

191. A.J. Mulac, W.L. Flower, R.A. Hill, D.P. Aeschliman, Appl. Opt. 17, 2695 (1978).

192. D.P. Aeschliman and R.E. Setchell, Appl. Spectr. 29, 426 (1975).

193. R.E. Setchell and D.P. Aeschliman, Appl. Spectr. 31, 530 (1977).

194. A. Leipertz and M. Fienig, Opt. Eng. 20, 599 (1981).

195. P.J. Hargis Jr., Appl. Opt. 20, 149 (1981).

196. P.J. Hargis Jr, Paper published in SPIE Proceedings Vol. 286 on Laser Spectroscopy for Sensitive Detection.

197. A. Weber, Ed. "Raman Spectrosocpy of Gases and Liquids". H.W. Schrötter and H.W. Klöckner in Chapter 4, Springer-Verlag, 1979.

198. R. Bailly, M. Pealat and J.P. Taran, Opt. Comm. 17, 68 (1976).

199. A. Leipertz, Opt. and Laser Techn. p 21, Febr. 1981.

200. D.L. Hartley, AIAA Journal 12, 816 (1974).

201. C.M. Penney, S.Warshaw, M. Lapp and M. Drake, p 247 in Ref. 86].

202. R.E. Setchell and J.A. Miller, Comb. and Flame 33, 23 (1978).

203. A.A. Boiarski, R.H. Barnes and J.F. Kircher, Comb. and Flame 32, 111 (1978).

204. R.J. Blint and J.H. Bechtel, J. Quant. Spectrosc. Rad. Trans. 23, 89 (1980).

205. M. Pealat, R. Bailly and J.-P. Taran, Opt. Comm. 22, 91 (1977).

206. M.C. Drake, M. Lapp, C.M. Penney, S. Warshaw and B.W. Gerhold, Paper presented at the 18th Symposium on Combustion, 17 Aug. 1980.

207. R.E. Setchell, "Initial Measurements Within an Internal Combustion Engine using Raman Spectroscopy", Sandia Report, Sand 78-1220, 1978.

208. C.R. Smith, AIAA paper 80-1359, AIAA 13th Fluid and Plasma Dynamics Conference, 1980.

209. S.C. Johnston, SAE Technical Paper Series 80136.

210. M.C. Drake and G.M.Rosenblatt, Chem. Phys. Lett. 44, 313 (1976).

211. M.C. Drake and G.M. Rosenblatt, Comb.and Flame 33, 179 (1978).

212. M.C. Drake and J.W. Hastie, Comb. and Flame 40, 201 (1981).

213. R.S. Hickman, A.E. Kassem and L.H. Liang, Appl. Spectr. 30, 179 (1976).

214. C.J. Barret and A.B. Harvey, J. Opt. Soc. Am. 65, 392 (1975).

215. C.J. Dasch and J.H. Bechtel, Opt. Lett. 6, 36 (1981).

216. M. Lapp, L.M. Goldman and C.M. Penney, Science 175, 1112 (1972).

217. M. Lapp, C.M. Penney and J.A. Asher, "Application of Light-Scattering Techniques for Meaurements of Density, Temperature and Velocity in Gas-Dynamics, Aerospace Research Laboratories, Wright-Patterson Air Force Base, Report No ARL 73-0045, 1973.

218. M. Lapp, C.M. Penney and L.M. Goldman, "Vibrational Raman Scattering Temperature Measurements", General Electric R & D Center, Technical Report No 73CRD224, 1973.

219. M. Lapp, C.M. Penney and L.M. Goldman, Opt. Comm. 9, 195 (1973).

220. A. Leipertz, Physik in unserer Zeit 12, 107 (1981).

221. G.F. Widhopf and S. Lederman, AIAA J. 9, 309 (1971).

222. M.C. Drake, M. Lapp, C.M. Penney and S. Warshaw, Paper presented at the AIAA 19th Aerospace Sciences Meeting in St. Louis, 1981.

223. M.C. Drake, M. Lapp and C.M. Penney, to be published in Temperature: Its Measurements and Control in Science and Industry, Vol. 5, Amer. Inst. Phys., New York, 1982.

224. W. Stricker, Comb. and Flame 27, 133 (1976).

225. D.A. Stephenson and W.R. Aiman, Comb. and Flame 31, 85 (1978).

226. R.A. Hill, A.J. Mulac and D.P. Aeschliman, J. Quant. Rad. Transf. 21, 213 (1979).

227. S.M. Schoenung and R.E. Mitchell, Comb. and Flame 35, 207 (1979).

228. G. Alessandretti, Optica Acta 27, 1095 (1980).

229. M. Lapp, p 107 in Ref. [82].

230. J.L. Bribes, R. Gaufrés, M. Monan, M. Lapp and C.M. Penney, Appl. Phys. Lett. 28, 336 (1976).

231. D.A. Stephenson and R.J. Blint, Appl. Spectr. 33, 41 (1979).

232. D.A. Stephenson, Appl. Spectr. 35, 582 (1981).

233. P.L. Hartley, p 311 in Ref. [82].

234. B.F. Webber, M.B. Long and R.K. Chang, Appl. Phys. Lett. 35, 119 (1979).

235. L.R. Sochet, M. Lucquin, M. Bridoux, M. Crunelle-Cras, F. Grase and M. Delhaye, Comb. and Flame 36, 109 (1979).

236. P.D. Maker and R.W. Terhune, Phys. Rev. A 137, 801 (1965).

237. A.B. Harvey, J.R. McDonald and W.M. Tolles, Progress in Analytical Chemistry 8, 211 (1976).

238. W.M. Tolles, J.W. Nibler, J.R. McDonald and A.B. Harvey, Appl. Spectr. 31, 263 (1977).

239. A.B. Harvey and J.W. Nibler, Appl. Spectr. Rev. 14, 101 (1978).

240. P.R. Regnier and J.P.E. Taran, Appl. Phys. Lett. 23, 240 (1973).

241. F.S. Moya, S.A. Druet and J.P.E. Taran, Opt. Comm. 13, 169 (1975).

242. P.R. Regnier, F. Moya and J.P.E. Taran, AIAA J. 12, 826 (1974).

243. A.C. Eckbreth and R.J. Hall, "CARS Diagnostic Investigations of Flames", Paper presented at the 10th Materials Res. Symp. on Characterization of High Temperature Vapors and Gases, NBS 1978.

244. J.P. Taran and M. Pealat, Paper presented on 6th Symposium on Temp., its Measurements and Control in Science and Industry, Washington 1982.

245. A.C. Eckbreth and P.W. Schreiber, "Coherent anti-Stokes Raman Spectroscopy (CARS): Applications to Combustion and Gas-Phase Diagnostics" in "Chemical Applications of Non-linear Raman Spectroscopy" A.B. Harvey, Ed. Academic Press 1981.

246. B. Attal, M. Pealat and J.P. Taran, J. Energy 4, 135 (1980).

247. R.L. St. Peters, "CARS:I. Introduction and Classical Radiation Theory", General Electric Corporate Research and Development, Report No 78CRD220, 1978.

248. R.L. St. Peters, "CARS:II. Simple Quantum Theory of Third-Order Polarization", General Electric Corporate Research and Development, Report No 78CRD249, 1978.

249. R.W. DeWitt, A.B. Harvey and W.M. Tolles, "Theoretical Development of Third-order Susceptibility as Related to Coherent anti-Stokes Raman Spectroscopy", NRL Memorandum Report, No 3260 (April 1976).

250. S. Druet and J.P. Taran in "Chemical and Biochemical Applications of Lasers" B. Moore, Ed. Academic Press, 1978.

251. S. Druet and J.P. Taran, Prog. Quant. Electr. 7, 1 (1981).

252. A.C. Eckbreth, Appl. Phys. Lett. 32, 421 (1978).

253. J.A. Shirley, R.J. Hall and A.C. Eckbreth, Opt. Lett. 5, 380 (1980).

254. Y. Prior, Appl. Opt. 19, 1741 (1980).

255. R.L. Farrow, P.L. Mattern and L.A. Rahn, Sandia Lab. Report SAND 80-8640 (1980).

256. D.A. Greenhalgh, "Comments on the Use of BOXCARS for Gas-phase CARS Spectroscopy", Harwell Report, AERE-R 10238 (1982).

257. W.B. Roh, P.W. Schreiber and J.P.E. Taran, Appl. Phys. Lett. 29, 174 (1976).

258. R.J. Hall, Comb. and Flame 35, 47 (1979).

259. W.M. Shaub, S. Lemont and A.B. Harvey, Computer Phys. Comm. 16, 73 (1978).

260. Th. Lasser, Opt. Comm. 35, 447 (1980).

261. R.L. St. Peters, Unpublished.

262. K.A. Markò and L. Rimai, Opt. Lett. 4, 211 (1979).

263. R.J. Hall and A.C. Eckbreth, Opt. Eng. 20, 494 (1981).

264. K. Muller-Dethlefs, M. Pealat and J.P.E. Taran, Ber. Buns. Phys. Chem. 5, 803 (1981).

265. L.E. Harris, Chem. Phys. Lett. 93, 335 (1982).

266. L.E. Harris and M.E. McIlwain, Comb. and Flame 48, 97 (1982).

267. I.R. Beattie, T.R. Gilson, D.A. Greenhalgh and J.D. Black, p 74 in Ref. [85].

268. A.C. Eckbreth and R.J. Hall, Comb. and Flame 36, 87 (1979).

269. M. Pealat, J.P. Taran and F. Moya, Optics and Techn. p 21 (Febr. 1980).

270. A.C. Eckbreth, Comb. and Flame 39, 133 (1980).

271. D.A. Greenhalgh, W.A. England and F.M. Porter, "The Application of Coherent anti-Stokes Raman Scattering to Turbulent Combustion Thermometry", Harwell Technical Report, AERE-R 10450, 1982.

272. I.A. Stenhouse, D.R. Williams, J.B. Cole and M.D. Swords, Appl. Opt. 18, 3819 (1979).

273. D. Klick, K.A. Marko and L. Rimai, Appl. Opt. 20, 1178 (1981).

274. L.A. Rahn, S.C. Johnston, R.L. Farrow and P.L. Mattern, "Temperature: Its Measurements and Control in Science ard Industry", 5, 609 (1982).

275. R.L. Farrow, P.L. Mattern and L.A. Rahn, Appl. Opt. 21, 3119 (1982).

276. M. Aldén and H. Edner, Unpublished.

277. M. Alden, S. Borgström, H. Edner, G. Holmstedt, T. Högberg and S. Svanberg, To be published.

278. R.J. Hall, J.A. Shirley and A.C. Eckbreth, Opt. Lett. 4, 87 (1979).

279. M. Aldén and H. Edner, Unpublished.

280. A.C. Eckbreth, R.J. Hall, J.A. Shirley and J.F. Verdieck, Fifth International Symp. on Airbreathing Engines, India (Febr. 1981).

281. M. Aldén, Unpublished.

282. J.W. Nibler, J.R. McDonald and A.B. Harvey, Opt. Comm. 18, 371 (1976).

283. V.V. Smirnov and V.I. Fabelinskij, JETP Lett. 28, 427 (1978).

284. M. Pealat, J.P.E. Taran, J. Taillet, M. Bacal and M. Bruneteau, J. Appl. Phys. 52, 2687 (1981).

285. T. Dreier, U. Wellhausen, J. Wolfrum and G. Marowsky, Appl. Phys. B 29, 31 (1982).

286. R.T. Lynch, Jr., S.D. Kramer, H. Lotem and N. Bloembergen, Opt. Comm. 16, 372 (1976).

287. F.M. Kamga and M.G. Sceats, Opt. Lett. 5, 126 (1980).

288. D.M. Guthals, K.P. Gross and J.W. Nibler, J. Chem. Phys. 70, 2393 (1979).

289. B. Attal, O.O. Schnepp and J.P.E. Taran, Opt. Comm. 24, 77 1978).

290. S.A Druet, B. Attal, T.K. Gustafson and J.P. Taran, Phys. Rev.A 18, 1529 (1978).

291. B. Attal, K. Muller-Dethlefs, D. Débarre and J.P. Taran, p 297 in Proceedings of the Eight International Conference on Raman Spectroscopy, J. Lascombe and P.V. Huong, Eds., Johr Wiley & Sons 1982.

292. B.Attal, K. Muller-Dethlefs, D. Debarre and J.P. Taran , Revue Phys. Appl. 18, 39 (1983).

293. L.A. Rahn, L.J. Zych and P.L. Mattern, Opt. Comm. 30, 249 (1979).

294. J.L. Oudar, R.W. Smith and Y.R. Shen, Appl. Phys. Lett. 34, 758 (1979).

295. A.F. Bunkin, S.G. Ivanov and N.I. Korotеev, Sov. Phys. Dokl. 22, 27 (1977).

296. A.C. Eckbreth and R.J. Hall, Comb. Sci. Techn. 25, 175 (1981).

297. L.P. Goss, J.W. Fleming and A.B. Harvey, Opt. Lett. 5, 345 (1980).

298. C.M. Roland and W.A. Steele, J. Chem. Phys. 73, 5919 (1980).

299. D.V. Murphy and R.K. Chang, Opt. Lett. 6, 233 (1981).

300. F. Moya, S. Druet, M. Pealat and J.P. Taran, p 549 in Ref. 83].

301. D.C. Smith and R.G. Meyerand, Jr., "Laser Radiation Induced Gas Breakdown", Chapter II in "Principles of laser Plasmas" G. Bekefi,Ed. Wiley-Interscience, New York (1974).

302. M.S. Chou, A.M. Dean and D. Stern, J. Chem. Phys. 76, 5334 (1982).

303. S.M. Schoenung and R.K. Hanson, Comb. Sci. Techn. 24, 227 (1981).

304. S.J. Harris and A.M. Weiner, Opt. Lett. 6, 142 (1981).

305. S.J Harris and A.M. Weiner, Opt. Lett. 6, 434 (1981).

306. J.E.M. Goldsmith, Opt. Lett. 6, 525 (1982).

307. J.E.M. Goldsmith and R.L. Farrow, Opt. Lett. 7, 215 (1982).

308. R.L. Farrow and L.A. Rahn, Opt. Lett. 6, 108 (1981).

309. K.C. Smyth, P.K. Schenck, W.G. Mallard and J.C. Travis, "Opto-Galvanic Spectroscopy: A new Look at Atoms and Molecules". Paper presented at the 10th Materials Res. Symp. on Characterization of High Temperature Vapours and Gases, NBS, 1978.

310. J.E. Goldsmith, Paper presented at the 1982 Fall Meeting of the Western States Section of the Combustion Institute, SANDIA, Livermore 1982.

311. J.E. Goldsmith, Opt. Lett. 7, 437 (1982).

312. K. Tennel, G.J. Salamo and R. Gupta, Appl. Opt. 21, 2133 (1982).

313. G.A. West and J.J. Barret, Opt. Lett. 4, 395 (1979).

314. W. Zapka, P. Pokrowsky and A.C. Tam, Opt. Lett. 7, 477 (1982).

315. J.R. Nestor, Appl. Spectr. 35, 81 (1981).

316. A. Owyoung, IEEE J. Quant. El. QE-14, 192 (1978).

317. L.A. Rahn and P.L. Mattern, p 76 in Ref. [85].

318. A. Owyoung and L.A. Rahn, IEEE J. Quant. El. QE-15, 25d (1979).

319. L.A. Rahn, Opt. Lett. 7, 66 (1982).

320. D. Heiman, R.W. Hellwarth, M.D. Levenson and G. Martin, Phys. Rev. Lett. 36, 189 (1976).

321. J.R. Smith, p 84 in Ref. [85].

322. R.W. Dibble and R.E. Hollenbach, Sandia Technical Report No SAND80-8623, 1981.

323. A. Leipertz, Appl. Opt. 21, 2872 (1982).

324. R.W. Pitz, R. Cattolica, F. Robben and L. Talbot, Comb. and Flame 27, 313 (1976).

325. P.A. Bonczyk, Comb. and Flame 35, 191 (1979).

326. J.B. Abbiss, T.W. Chubb and E.R. Pike, Optics and Laser Techn. p 249 (Dec. 1974).

327. R.L. Byer, Opt. Quant. Electr. 7, 147 (1975).

328. E.D. Hinkley, Ed., "Laser Monitoring of the Atmosphere, Topics in Applied Physics", Vol. 14 Springer Berlin-Heidelberg, 1976 .

329. R.M. Measures in "Analytical Laser Spectroscopy", N. Omenetto Ed., J. Wiley & Sons N.Y., 1979 .

330. S. Svanberg, Contemp. Phys. 21, 541 (1980).

331. K. Fredriksson, "Laser Spectroscopy Applied in Studies of Alkali-atom Structures and in Environmental Monitoring", Ph.D. dissertation, U. Gothenburg (1980).

332. K. Fredriksson, "Conclusion from the Evaluation and Testing of the Swedish Mobile Lidar System, Swedish National Environment Protection Board Report, SNV PM1639, 1983.

333. K. Fredriksson, I. Lindgren and S. Svanberg, Proceedings of the Fourth Joint Conf. on Sensing of Env. Pollutants, New Orleans, Nov. 6-11, 1977.

334. K. Fredriksson, B. Galle, K. Nyström and S. Svanberg, Appl. Opt. 18, 2998 (1979).